University of Nevada, Reno

Feasibility and Implementation Plan for Rainwater Harvesting in Peach Springs, AZ on the Hualapai Indian Reservation

A thesis submitted in partial fulfillment of the
Requirements for the degree of Master of Science in
Hydrogeology

by

Brianda Hernandez Rosales

Dr. Alexandra Lutz, Thesis Advisor

May, 2022

THE GRADUATE SCHOOL

We recommend that the thesis
prepared under our supervision by

BRIANDA HERNANDEZ

entitled

Feasibility and Implementation Plan for Rainwater Harvesting in Peach Springs, AZ on the Hualapai Indian Reservation

be accepted in partial fulfillment of the
requirements for the degree of

MASTER OF SCIENCE

Alexandra Lutz, Ph.D.
Advisor

Christine Albano, Ph.D.
Committee Member

Susan Rybarski, M.Sc.
Graduate School Representative

David W. Zeh, Ph.D., Dean
Graduate School

May, 2022

Abstract

The strain on available freshwater resources has increased during the past century. With nearly half of the global population, roughly 4 billion people, living in conditions of severe water stress for part of the year and with expected climate change in the coming decades, finding additional renewable water resources is crucial to ensure safe drinking water and attain food security. Rainwater harvesting (RWH), the practice of centralizing, collecting, and storing rainwater for later use, has the potential to help alleviate some water stresses in rural communities. Although RWH is not a new concept, it has not been widely practiced in arid and semi-arid environments in the United States. This study assesses the feasibility of rooftop RHW at a small scale, in Peach Springs, Arizona, on the Hualapai Indian Reservation. Working alongside the Federally Recognized Tribal Extension Program (FRTEP) agent for the Hualapai Tribe, this study considers RWH from four prospective buildings to supplement irrigation practices for food production. An average total of ~28,141 liters can be collected from one of the buildings considered for RWH during the growing season of April to September. Annual precipitation amounts were classified into normal, dry, and wet years to assess variability over the last 41 water years. The study indicated that more precipitation is accumulated during the winter, rather than summer, months of a wet year compared to a normal or dry year, where most precipitation is falling during the monsoonal months of July and August. The Food and Agriculture Organization's (FAO) AquaCrop model was used to determine the area that can be cultivated by four staple crops -maize, tomatoes, dry beans, and sunflowers- that are currently being grown in the community garden, solely using the captured rainwater.

Cultivable areas range from 8.7 m^2 to 71 m^2 depending on the catchment size, crop, and classified precipitation year — wet, dry of normal precipitation year. A total of 81.2 kg of dry corn can be harvested during a normal precipitation year, solely using the collected rainwater. Climate projections for Peach Springs show an increase in average daily temperature which will lead to higher reference evapotranspiration (ETo), resulting in more water needed to sustain a healthy crop yield. Temperature increases and variability in precipitation shown in the climate projections could have an intense effect on crop yields in the Southwest.

Acknowledgements

I would like to thank my advisor Dr. Alexandra Lutz for being the best mentor and teacher of hydrology that I could have ever asked for during this graduate degree. Her support of students and dedication to addressing water security for underserved communities is an inspiration and I am grateful to have learned and continue to learn from her. I would also like to thank the other amazing scientists on my committee, Dr. Christine Albano for sharing her expertise and time to investigate the climate projections for this project, and Susie Rybarski for her support and for asking the fundamental questions needed for me to conduct better science. I would like to thank Federally Recognized Tribal Extension (FRTEP) Agent, Elisabeth Alden, for her interest in this project, as well as the Hualapai Tribe for granting us the opportunity to conduct this research and visit their homelands during an unprecedented time. This project would not have been possible without the support from the Desert Research Institute's Lander Endowment Research Fund, Sean McKenna, and Tim Minor.

Contents

List of Tables

List of Figures:

1.0 Introduction

The strain on available water resources has increased during the past century (Kummu et.al., 2010). Nearly half of the global population, roughly 4 billion people, live in conditions of severe water stress for part of the year (Mokonnen et al., 2016). In the United States, approximately 130 million people, particularly in western states, live in water stressed conditions for at least 1-6 months out of the year (Mekonnen et al., 2016). Climate variability is likely to increase in the coming decades. Increasing temperatures and changes in precipitation variability have potential to intensify already stressed water resources and creating conditions of water insecurity.

Access to clean, reliable water is a basic human right. However, the lack of water security is exacerbated in some places, particularly rural and tribal communities (DigDeep & US Water Alliance, 2020). In the southwestern United States (US), 40% of households in the Navajo Nation lack access to running water, an astonishingly low number at a time when constant handwashing is needed to help slow the spread of the COVID-19 (Power et al., 2020; Wilson et al., 2021). Expanding water portfolios in these communities can help address water security, especially for drinking, hygienic practice, and food production.

Rainwater harvesting (RWH), which includes concentrating, collecting, and storing rainwater in small schematic systems for domestic and agricultural use (Lesage & Verburg, 2014), is a sustainable water resource that has been practiced for centuries to address water security in arid and semi-arid environments around the world (Van Meter et al., 2016). Apart from Tucson, Arizona, RWH has yet to be

widely studied and implemented in much of the southwestern US, particularly in Arizona. There, RWH can be a viable and attainable solution to address water security issues in the rural areas where connectivity to water mains is impossible due to the large distance between homes and lack of infrastructure (DigDeep & US Water Alliance, 2020). The feasibility and implementation of RWH systems in these underserved communities are an understudied research topic that is especially important as climate variabilities are anticipated to increase.

Rainwater harvesting requires minimal engineering and construction, low cost, and maintenance all while collecting water that can support outdoor purposes, particularly, irrigation for crop production. Studies have shown that RWH is not only feasible in wet climates, but in arid and semi-arid climates as well, which can improve rain-fed farming systems (Tamaddun, 2018). Additionally, RWH can be the solution needed to manage increasing water demands, water scarcity and climate variability as another source of clean water (Durodola, 2020).

This study aims to assess the feasibility of rooftop RWH from four buildings on the Hualapai Indian Reservation in Peach Springs, AZ, by characterizing the current and future climatic patterns, determining the potential volume that can be captured based on 40-year climatic data, investigating the area that can be cultivated using the AquaCrop model and determining the costs of implementing the project. The following questions are addressed:

1. Do current Peach Springs climate patterns support feasibility of RWH and does this change with future climate projections?
2. Are the existing rooftops on the four proposed buildings well-suited for rooftop RWH and how much volume could be harvested?
3. How much land area can be cultivated using the harvested rainwater and would a dry year still be sufficient to sustain the crops?

2.0 Literature Review

2.1 Study Area

The study area is focused on the town of Peach Springs, located in the northwestern corner Arizona on the Hualapai Indian Reservation (Figure 1). The Hualapai Indian Reservation, which was established in 1883, straddles the Mohave and Coconino counties. The Hualapai Indian Reservation encompasses 4,046 km² along the lower end of the Grand Canyon and Colorado River (HTDNR, 2004) with two additional satellite areas of the reservation near Valentine, AZ and Wikieup, AZ — both averaging around 3.9 km² in size (Christensen & HTDNR, 2003). The u-shaped reservation is bordered by the Grand Wash Cliffs to the west, the Colorado River to the north and the Havasupai Reservation to the far east (UACE, 2008).

The town of Peach Springs —35.529125 latitude and -113.425461 longitude— sits about 80 km northeast of Kingman, AZ and approximately 1,457 m in elevation, is the headquarters for the Hualapai Tribe. The town of Peach Springs has an area of 20.5 km² and a population of 1,500. It is the main town in the Hualapai Indian Reservation and is cut by the iconic Route 66 (NPS, 2021). The Burlington Northern and Santa Fe Railway (BNSF) travels slightly south of Route 66 through the southern end of the Reservation. In 1978 Interstate 40 bypassed the town of Peach Springs, slowing down tourism-based economic opportunities on the reservation (UACE, 2008). However, Peach Springs serves as the gateway to various attractions along the Colorado River including the Grand Canyon West and the famous village of Supai, on the Havasupai lands (UACE, 2008).

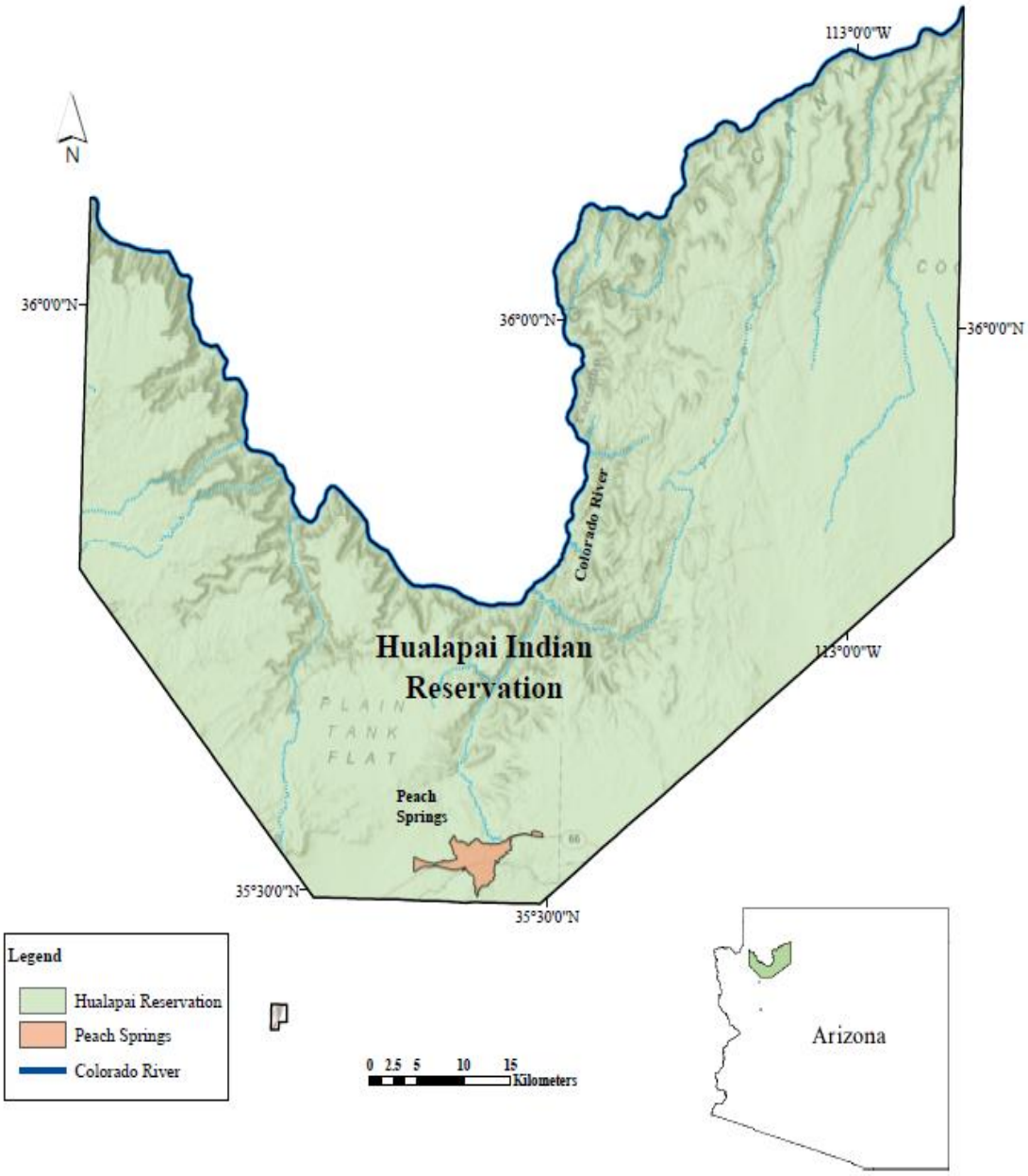

Figure 1 | The study area in the town of Peach Springs on the Hualapai Reservation in northwestern Arizona

Service Layer Credits: National Geographic, Esri, Garmin, HERE, UNEP-WCMC, USGS, NASA, ESA, METI, NRCAN, GEBCO, NOAA, increment P Corp.

2.2 Hualapai Tribe

The Hualapai, “People of the Tall Pines,” are a federally recognized tribe with over 2,300 tribal members of which 1,500 live within the reservation boundary (HDCR, 2010). The Hualapai live on a small fraction of their ancestral lands that once encompassed over 20,000 km² in Northwestern Arizona (HDCR, 2010). The prominent location of the Hualapai Reservation has ensured the successful living of the people within the reservation (HDCR, 2010). With abundant resources that consist of hunting, gardening, and the collection of native plants, roots, minerals and rocks, the Hualapai have flourished in the far northwestern edge of the Colorado Plateau (HDCR, 2010). The Hualapai Reservation is rich in a variety of vegetation, which includes native plants consisting of desert tobacco, cane, reed, bear grass, various cacti, and grass seeds (HDCR, 2010).

The Hualapai Tribe’s main economic activities include tourism, cattle ranching, and arts and crafts. The Hualapai Tribe welcome an abundance of visitors every year to their Grand Canyon West location. The Hualapai River Runners also see many recreational enthusiasts every year. The Hualapai Community Garden is located next to the Hualapai Cultural Center and managed by Federally Recognized Tribal Extension Program (FRTEP) agent, Elisabeth Alden, and tribal members. The garden has an array of vegetables, fruits, and herbs, including tomatoes, corn, squash, cucumber, zucchini, sunflowers, strawberries, and peppers. The provisions are for the tribal members at no additional costs.

2.3 Climate

The climate on the Hualapai Reservation is characterized as mild and arid (Christensen & HTDNR, 2003). There are two rain gauge stations on the reservation. One is near Peach Springs with a record period from 1948-2006 and the other near the town of Truxton, located slightly southwest of the town of Peach Springs, with a record period from 1901-1980; both stations record an average annual precipitation of about 279 mm (Bills & Macy, 2016). However, according to the climate normal from 1990-2020, mean annual precipitation has fallen to 245 mm per year. Most of the precipitation on the reservation is received during the monsoonal months of July and August and during the cooler months of December, January and February (Figure 2). Snow accumulations occur at higher elevations during the winter months (Christensen & HTDNR, 2003). The mean

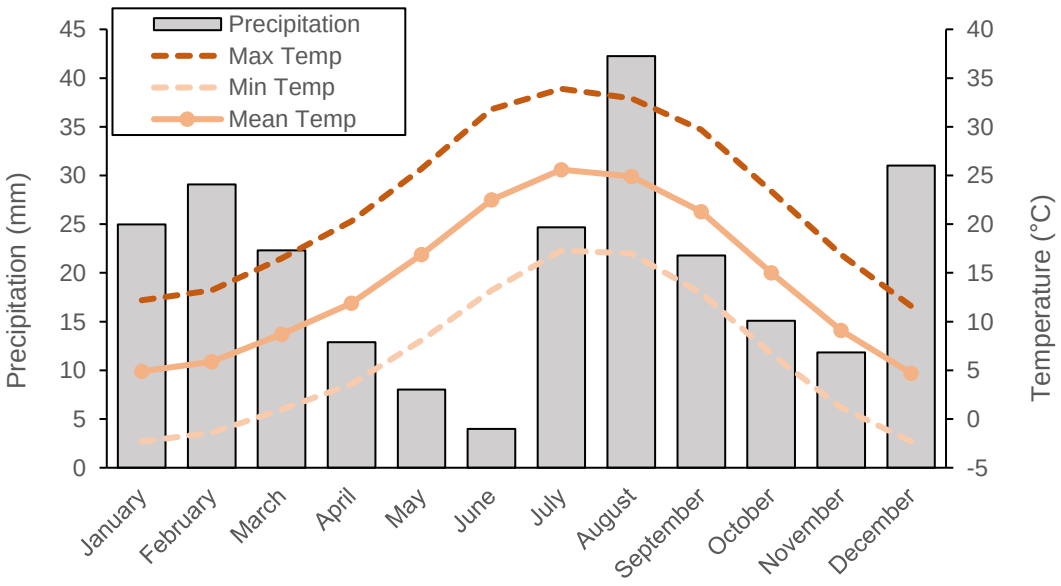

Figure 2 | Monthly normals for Peach Springs, AZ from 1980-2010 using PRISM precipitation and temperature data. Climate normals are baseline datasets recounting average climatic measurements from 1980-2010

temperatures are 23 °C in the summer and 6 °C during the winter according to the climate

normals from 1990-2020. Maximum and minimum temperatures have been recorded at 44 °C and -17 °C, respectively, in Peach Springs, AZ (Bills and Macy, 2016).

The reservation experiences frequent episodes of droughts that can last several years followed by shorter periods of above normal to extreme wet weather conditions (Bills & Macy, 2016). Currently, the reservation along with much of the southwestern US is experiencing a long-term drought, referred to as a megadrought, which began in the late 1990's, early 2000s (Williams, et al., 2022). During 1995-2006 annual precipitation recorded at Peach Springs was less than average (Bills & Macy, 2016) and there has been no observational meteorological data recorded since 2007. Kohler et al., (1959) determined potential evaporation estimates of 1.5-1.7 m per year, exceeding the annual precipitation of 279 mm per year making the basin energy dominant. Another study looking at evaporation rates for the Southern Colorado Plateau estimated potential evaporation rates at 1.7–2.0 m per year in the region (Wang et al., 2020).

2.3.1 North American Monsoon

The North American Monsoon (NAM) also known as the Southwest monsoon, Arizona monsoon or the Mexican monsoon (Adams and Comrie, 1997) brings an abundance of rain to northwest Mexico and the southwestern US every summer (Pascale et al., 2017; Adams and Comrie, 1997). Although there has been a decent amount of research on the NAM, the mechanism and characteristics behind the monsoon are yet to be entirely understood. The NAM precipitation is suggested to be composed of two primary moisture sources — the Pacific Ocean through the Gulf of California and the Gulf of Mexico (Perez Quezadas et al. 2021; Dominguez et al. 2016), however, recent

studies have shown that terrestrial water sources along with the water vapor sources form the Gulf of California are the leading sources for precipitation in the summer months (Perez Quezadas et al. 2021). The NAM starts in western Mexico in the month of June and makes its way to the southwestern US by July and lasting as late as mid- September (Adams and Comrie, 1997). The NAM is a result of various convective thunderstorms that form from surface land heating and moisture (Crimmins, 2006). Many variables influence the creation and intensity of the monsoon. As a result, summer precipitation patterns vary widely from year to year, which is associated with the conditions of the Pacific Decadal Oscillation and the El Nino Southern Oscillation (ENSO) (Copeland et al., 2017).

The NAM, however, might be experiencing a weakening in recent years due to global warming (Pascale et al. 2017). The NAM's response to increasing greenhouse gases remains unclear, but models are showing that there may be a decrease in precipitation during the months of June and July, and an increase in precipitation intensity during the later months of the monsoon —September and October (Pascale et al. 2017). Furthermore, uncertainty adheres to these results, indicating that further research needs to be done to conclusively predict its future characteristics.

2.4 Geology

Sitting on the southwestern edge of the Colorado Plateau Province, the geology of northwestern Arizona is a medley of Proterozoic to Quaternary rock formations. The Hualapai Reservation lies mostly atop the Hualapai Plateau (Figure 3) with a minor portion of the eastern side of reservation on the Coconino Plateau — both sub-provinces of the Colorado Plateau (Bills & Macy, 2016). The geology of the Hualapai Plateau consists of Mississippian, Devonian, and Cambrian sedimentary rocks with pockets of more recent—Quaternary and Tertiary— surficial deposits (Mason et al.(a), 2020). Proterozoic crystalline and metamorphic rocks form the basement lithologies of the plateau. Within the southeastern edge of the plateau lies the Truxton basin, an ancient drainage and topographic depression approximately 194 km² in size. The Truxton basin and the Hualapai plateau are believed to be once geologically similar to one another, however the Laramide uplift in the Late Cretaceous and Paleogene lead to erosion of all the Mesozoic and Paleozoic deposits in the Truxton basin (Mason et al.(b), 2020). The Truxton basin is filled with Quaternary and Tertiary basin fill deposits with occasional Cambrian rock formations (Mason et al.(b), 2020). The Hurricane Fault is a west dipping normal fault trending northeast to southwest through southwestern Utah and northwestern Arizona (Stenner et al., 1999). The 280 km long Hurricane Fault directly cuts the Truxton basin in half.

Peach Springs lies to the east of Hurricane Fault and on the eastern edge of the Truxton basin. Local geology is comprised of Mississippian, Devonian, and Cambrian sedimentary rocks. To the east of Peach Springs and on the far eastern edge of the

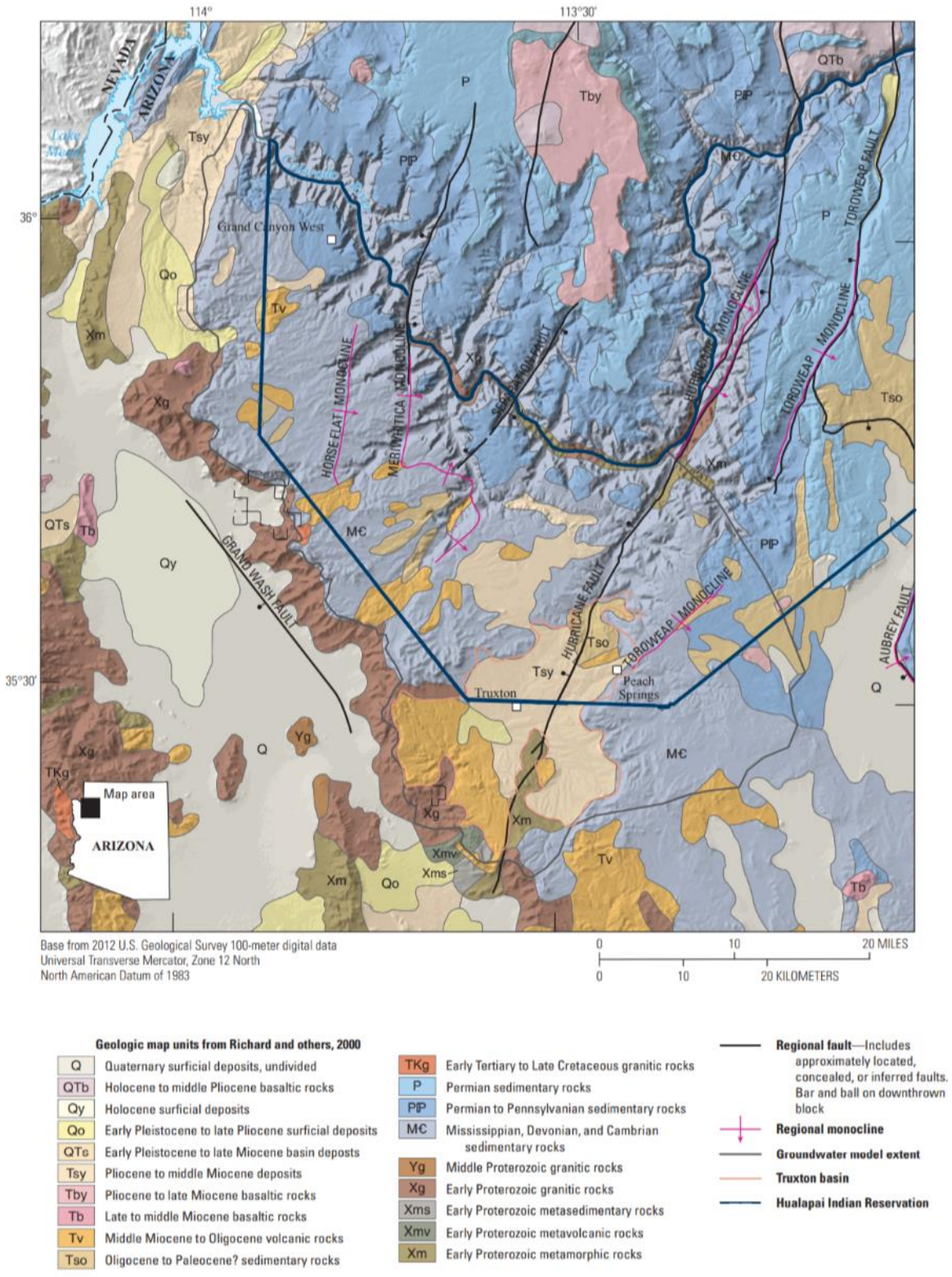

Figure 3 | Geology of the Hualapai Reservation in northwestern Arizona (modified from Mason et al., 2020, USGS).

reservation, the Coconino Plateau envelops the area. The geology of the northwestern

edge of the Coconino Plateau is dominated by Precambrian granitic and metamorphic rocks at the base as well as Paleozoic and Mesozoic rocks, Tertiary and Cenozoic volcanic rocks (Bills et al., 2016) and Cambrian sedimentary rocks (Moore et al., 1960) at the surface. This study area is focused mainly on the Hualapai plateau and Truxton basin.

2.5 Hydrology and Hydrogeology

Due to the location, sparse population, and water use of the area along with the limited available flow data for both surface and groundwater, the hydrology and hydrogeology on the Hualapai Reservation is not completely understood (Bills & Macy, 2016). Most of the surficial water drainages on the reservation are ephemeral, only flowing during high intensity precipitation events (Mason et al, 2020a; Bills & Macy, 2016). However, some drainages flowing year-round are supplemented by the groundwater discharge from springs (Mason et al.(a), 2020; Bills & Macy, 2016). These perennial streams are usually discharged from very remote springs, making the gage and water quality data difficult to attain (Bills & Macy, 2016). The reservation, in cooperation with the United State Geological Survey (USGS), monitor and maintain three stream gauge stations on the reservation: Diamond Creek, Spencer Canyon, and the Truxton wash (HDNR, 2021).

The Truxton wash is the main drainage of the Truxton Basin. The Truxton Wash is an ephemeral stream starting in the Yampai Cliffs in the Yampai and Nelson Canyons located east of the Truxton basin (Bills & Macy, 2016). The Peach Springs wash is

ephemeral at its headwaters in the town Peach Springs but is then supplemented by groundwater from the Peach Spring to the Peach Springs Canyon, allowing for year-round flow of about 1.73 $x10^5$ m^3 (141 ac-ft). Peach Springs wash becomes ephemeral once again after the Peach Springs Canyon (Bills & Macy, 2016). Spencer Creek, on the northern edge of the reservation, is also a perennial drainage. The main source of Spencer Creek originates from springs off the Rampart Cave Member of the Mauv Limestone (Mason et al. 2020b) in Spencer Canyon. Diamond creek also originates from springs deep in a canyon on the Coconino Plateau (Mason et al. 2020b).

Multiple studies conducted by the USGS, Mason et al., 2020a, and Bill and Macy 2016, as well as private consulting firms hired by the Hualapai Tribe attempt to understand the hydrogeology of the Hualapai Reservation. The Truxton aquifer is the main source for groundwater for the Tribe and is situated near the southern boundary of the reservation. It is understood that the Truxton basin was once part of an ancient drainage and paleo-canyon that eroded after the Laramide uplift of the southwestern Colorado Plateau approximately 70-40 million years ago. Erosion exposed the surface of Proterozoic and Paleozoic rocks that lie beneath the Truxton basin, southwest to northeast at an angle of 1-3° (Mason et al., 2020a). Forming the Truxton aquifer are mainly poorly sorted medium to coarse-grained sediments with some amounts of clay (Mason et al., 2020a). The younger basin-fill at the surface in the Truxton basin is unsaturated but has moderate permeability. Near the town of Peach Springs, groundwater is found at approximately 610 m below the surface in the Mauv Limestone (Bills and Macy, 2016).

Inflow to the basin enters mainly through underflow and mountain front recharge from the Music Mountains on the Hualapai Plateau (Mason et al., 2020b). Recharge to the aquifer is estimated at 3.63×10^5 m³ (295 ac-ft) per year from mountain front recharge and approximately 2.5×10^6 (2,000 ac-ft) from underflow from adjacent aquifers (Knight. 2020). Minimal surficial recharge is believed to enter the Truxton aquifer due to low precipitation and high evaporation rates (Mason et al., 2020a). The Truxton wash serves as the outflow conduit for the Truxton basin along with underflow from the north of the basin and withdrawals from the Truxton well field also serve as an outflow (Mason et al., 2020b). Although the Truxton aquifer has porosity and permeability characteristics conductive to the groundwater production, the recharge rate limits the groundwater outflow from the Truxton basin, at 7.21×10^5 m³ (585 ac-ft) per year from withdrawals and the Truxton wash (Bills and Macy, 2016) with an additional underflow to adjacent aquifers at approximately 2.5×10^6 (2,000 ac-ft). The annual outflow is approximately larger than the inflow by close to 3.7×10^5 (300 ac-ft), additionally, it is expected for water withdrawals to double in the coming decades as population and water demand increases, making a long-term dependence on the aquifer unsustainable.

2.6 Rainwater Harvesting

Rainwater harvesting refers to the practice of concentrating, collecting, and storing of rainwater in small schematic systems for domestic and agricultural use (Lesage & Verburg, 2014). It is a sustainable water resource that has been practiced for centuries to address water scarcity in arid and semi-arid environments around the world (Van Meter et. al., 2016). It can be used to alleviate the stresses of both surface and groundwater resources in semi-arid and arid places. In addition, RWH can be used for both non-potable and potable use. Non-potable water can be used directly for agriculture and livestock drinking water by various methods (Figure 4). Potable use of rainwater, however, requires regulations and additional filtration. This study will focus on the feasibility of non-potable agricultural or outdoor use of rooftop RWH, from four buildings on the Hualapai Indian Reservation: the 4H building, the tractor shed, the toolshed, and the greenhouse.

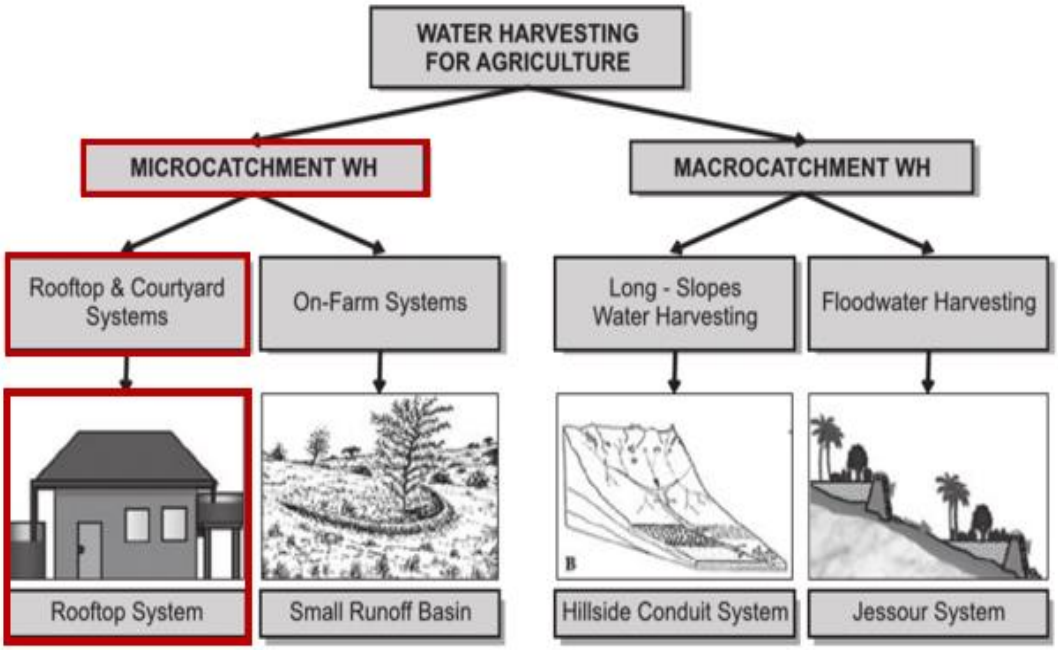

Figure 4 | Methods for rainwater harvesting for agricultural use (Modified from Oweis et al. 2012). This study will focus on rooftop rainwater harvesting micro-catchments (red).

Rooftop RWH is a small-scale application that can be as simple as diverting rain from gutters into a rain barrel for outdoor use. The application requires the following basic components detailed by the Texas Manual on Rainwater Harvesting by the Texas Water Development Board (2005):

- Catchment surface: A surface where rainwater can be collected from
- Gutters and downspouts: Used to channel rainwater to a specific location
- Leaf screens and first flush diverters: Allows for larger debris to be filtered out and the existing contaminants on the roof be flushed out
- Storage tanks or cisterns to store the collected rainwater for later use
- Delivery system: gravity fed or pumped to the end use

These simple components make rooftop RWH a viable and cost-effective solution to water scarcity worth considering. Rooftop RWH will just be referred to as RWH for the remainder of this study.

2.7 AquaCrop Model and Evapotranspiration (ET)

The AquaCrop Model was developed by the Food and Agriculture Organization (FAO) Land and Water Division to address limitations facing end users who are trying to determine potential crop yield in relation to available water. Most crop models require a substantial number of inputs and parameters that may be too extensive for the model's end users or not readily available (Vanuytrect et al., 2014). AquaCrop uses a simple, accurate and straightforward approach, requiring a small number of explicit parameters and intuitive input variables that can be easily attained by any user of the model (Durodola et al., 2020; Vanuytrect et al., 2014). These inputs and parameters include precipitation, temperature, reference evapotranspiration (ETo), crop and soil information. AquaCrop is a multi-crop model, allowing the user to adopt one of the calibrated default crops (maize, tomatoes, potatoes, wheat, etc.) or input calibrated information about a desired herbaceous crop.

Evapotranspiration (ET), the process by which liquid or solid water on the Earth's surface becomes atmospheric water vapor, due to evaporation from the land surface and transpiration from plants, is important to understand for crop production (Dingman, 2015). Further information about a plant's physiology and ET can be found in Dingman (2015). Reference evapotranspiration (ETo) represents the growing conditions for a grass

crop under optimal growing conditions (Figure 5), mainly referring to the availability of water (Raes, 2012). ETo is used alongside crop coefficients (Kc) to estimate the amount of water a crop is transpiring which can determine how much water the crops need for irrigation. Further information about the role of ETo and crop production can be found in Allen et al (1998) and Raes et al (2012). ETo is a climatic parameter, so it can be easily calculated from weather data, by using the FAO Penman- Monteith method, which has been selected as the primary method because procedures have been developed to assess and estimate missing climatic information (Allen et al., 1998).

The FAO's ETo Calculator program uses the Penman- Monteith equation to determine ETo by assessing meteorological data (FAO, 2022). The ETo Calculator program uses daily, ten-day, and monthly climatic data (e.g., precipitation, temperature, wind speed and solar radiation). The program uses specific procedures to estimate for any missing climatic data and conditions. The ETo calculator was developed to help agrometeorologist, agronomist, and irrigation managers calculate ETo to be used in crop water demand research (FAO, 2022). The program is readily accessible, user friendly, and adaptable. It can export information into text files or be directly input in the FAO's AquaCrop model (section 3.4). Further information about the FAO ETo Calculator can be found in the reference manual version 3.2 (Raes, 2012). The AquaCrop model focuses on water management since that is the central aspect in crop production at any scale. Crop watering methods and amounts can be input by choosing two different water management options: rainfed agriculture (no irrigation) and irrigation with three application methods (sprinkler, drip, and surface). The model allows for inputs of time and depth of the desired irrigation method. Additionally, the model allows for an automatically generated

net irrigation which includes fixed time intervals, fixed irrigation amounts needed for the specific crop, or a percentage of allowable water depletion in the crop and soil (Steduto et al., 2009). Net irrigation is the total amount of water required to maintain the water content in the soil profile at an ideal state to avoid stressing the crop (Raes, et al., 2013). Maize, tomatoes, beans, and sunflowers, or a variation of these crops, are staple fruits, vegetables, or grains in the Southwest (Guarino, 2015). This study will focus on these crops.

AquaCrop links the growth to available water by the two water management methods -rainfed or irrigation- to simulate the potential yield for a specific crop. The model estimates biomass production from ETo through a normalized productivity parameter and simulates the soil-water balance and crop growth processes with crop, soil, climate, and water management inputs (Durodola et al., 2020). Input files are contrived into ‘projects’ that allow for 11 different input data and can be modified through a simple user interface. The simulated results are then recorded as text files and can be grouped into 10-day, monthly, or annual summaries.

Five output files consisting of the simulated crop growth and production, soil-water balance, soil water content at various depths and the net irrigation requirements to acquire the desired crop yield, can be acquired. The ease of use of the model, minimal input parameters and ample degree of simulation accuracy, makes the model a substantial tool in determining the net irrigation and crop yield for this study. Further information

about AquaCrop has been reported by others (Vanuytrect et al., 2014; Steduto et al., 2009).

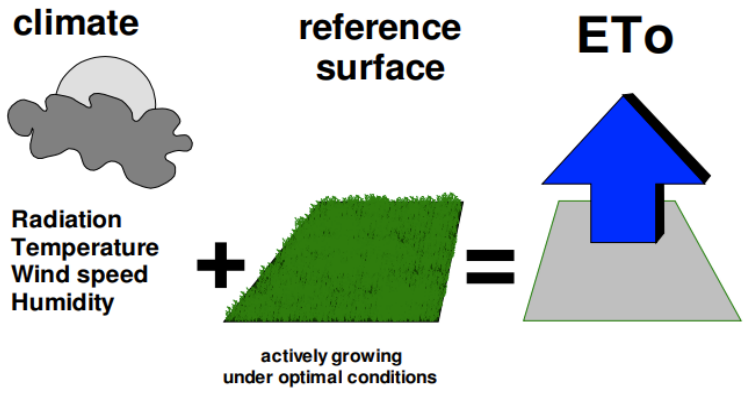

Figure 5 | Schematic figure of reference evapotranspiration (ETo), representing the growing conditions for grass crop under optimal growing conditions. Figure from Raes, 2012

2.8 Food Security and Sovereignty

Both COVID-19 and climate change have exacerbated food insecurities worldwide. An estimated 821 million people, globally, experienced hunger (e.g., chronic food insecurity, undernutrition, and malnutrition) in 2018 and it is suggested that the number will grow due to the ongoing global pandemic (Congressional Research Service 2020). The US Food and Drug Administration (USDA) has determined that approximately 10.5% of Americans live in food-insecure households (Figure 6), which include low food security (6.6%) and very low food security (3.5%), where low-food security refers to food-insecurity without hunger, meaning that individuals face reduced

food quality, variety and desirability of diet, in comparison to very low food security where food insecurity is experienced with hunger, meaning individuals report disrupted eating patterns and reduced food intake (USDA, 2020). A study published by Myers and Painter (2017) reported that people of color are disproportionately affected by the health impacts regarding insufficient and poor-quality foods which include higher rates of cardiovascular diseases, diabetes, obesity, hypertension, as well as affecting mental and developmental health. The 2000-2010 "Current Population Survey Food Security Supplement" reported that 25% of American Indians and Alaskan Natives remain food insecure compared to white Americans, highlighting the prevalence of food security and the need to find ways to address food security, food access, and nutritional needs in tribal communities and rural areas (Pindas and Hafford, 2017).

Approximately 85% of residents on most Native American reservations receive food assistance through the USDA's Food Distribution Program on Indian Reservations, unfortunately, foods distributed through this program tend to consist of prepackaged and canned foods that are high in salts, sugars, and fats (Blue Bird, Jernigan et al. 2011). The inability to access fresh and healthy foods has led tribal communities to an increase in health disparities including cardiovascular diseases, diabetes, and cancer (Warne and Wescott, 2019; Pindas and Hafford, 2019; Blue Bird Jernigan et al., 2011).

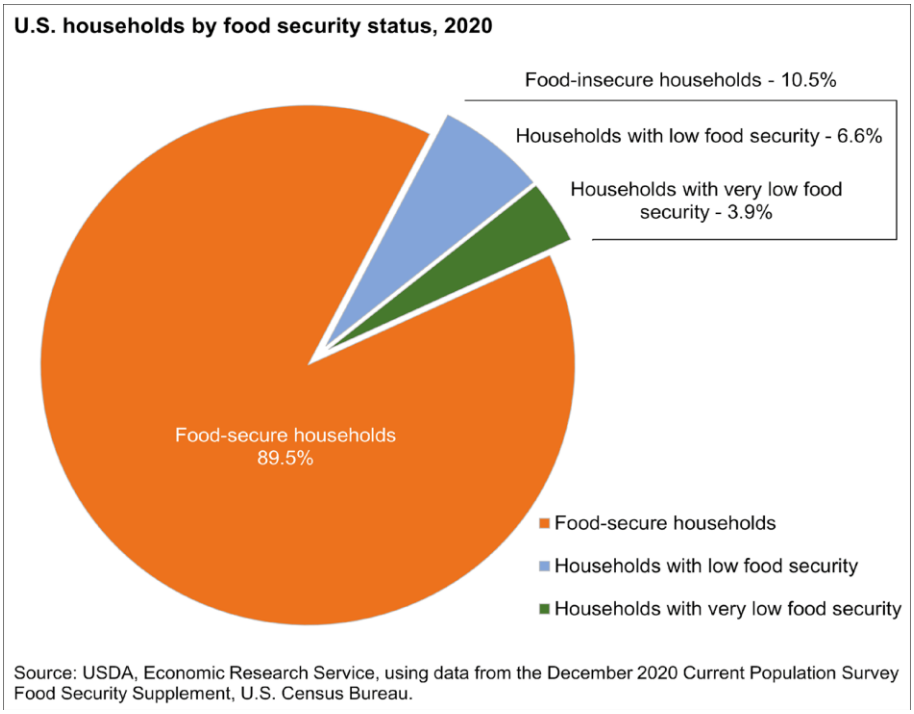

Figure 6 | Food security chart in the United States where 10.5% of Americans endure low to very low food-insecurities (Coleman-Jensen et al., 2020).

The term 'food sovereignty' was introduced at the World Food Summit to make aware the disparities in food production and to support locally grown, sustainable food among indigenous peoples, migrants, agricultural workers, women farmers, and small to medium-sized farm, further elaborating the meaning behind the term to include:

> Food sovereignty is the right of peoples to healthy and culturally appropriate food produced through ecologically sound and sustainable methods, and their right to define their own food and agriculture systems. It puts the aspirations and needs of those who produce, distribute, and consume food at the heart of food systems and policies rather than the demands of markets and corporations

(La Vía Campesina, 2007)

Access to healthy, beneficial, and cultural foods can lead to the strengthening of cultural identity and strengthen their relationship to their ancestral lands (Pindas and Hafford, 2019). By attaining food security and food sovereignty, tribal communities will be able to connect back to traditional foods and practices which in turn can improve their health. To attain this goal, ensuring water security for food production is essential.

3.0 Methods

3.1 Field Methods

Field observations were conducted in August 2021 in Peach Springs under the guidance of the Hualapai Tribe's FRTEP agent Elisabeth Alden. Measurements of the 4H building, the greenhouse, the toolshed, and the tractor shed were taken with a handheld measuring tape. Additionally, a survey of the crops in the Hualapai Community Garden was taken, which included the type of crops, the time of sowing and the time of harvesting and the soil characteristics. Lastly, an inventory was taken of the existing material that has the potential to be used for RWH to help determine a cost budget. Field data, additional photographs of the four buildings, crops in the current community garden, and existing material can be found in Appendix (8.1).

3.2 Climate Characterization

3.2.1 Time Series Analysis

Monthly and annual precipitation and temperature information from 1980 to 2020 were downloaded from PRISM Climate Group at 4 km resolution (PRISM, 2021) for the town of Peach Springs. The R programming code was used to calculate mean annual precipitation, standard deviation, coefficient of variation, skewness, and a decomposition time series analysis.

The coefficient of variation (CV) is a measure of relative variability and calculated as:

$$CV = \frac{S_d}{V_a} \quad [1]$$

where CV is the coefficient of variation, S_d is the standard deviation of monthly precipitation (mm) and V_a is the mean of monthly precipitation (mm). Interannual CV was calculated for the years from 1980-2020. Skewness describes data sets that are not symmetric around the mean, with values extending out longer in one direction as compared with another (Helsel and Hirsch, 2002).

A decomposition time series analysis using the decompose function in R, breaks down the data into seasonal, random, and trend components for monthly precipitation from 1980-2020. Here, decomposition of the precipitation time series reduces "noise" that can obstruct results, allowing for a cleaner view of precipitation and temperature trends and better understanding any problems with the time series and forecasting. A multiplicative decomposition of a time series was employed:

$$Yt = Tt \times St \times Rt \quad [2]$$

where Yt is the time series, Tt is the trend component, St is the seasonality component and Rt is the remainder or noise of the time series. A multiplicative decomposition was chosen instead of an additive decomposition due to the seasonal variation in precipitation increasing over time. Additionally, locally weighted scatterplot smoothing (LOWESS)

was used to discern the direction of both the precipitation and temperature trends. A smoothing tool can help generalize the direction of a trend, if present.

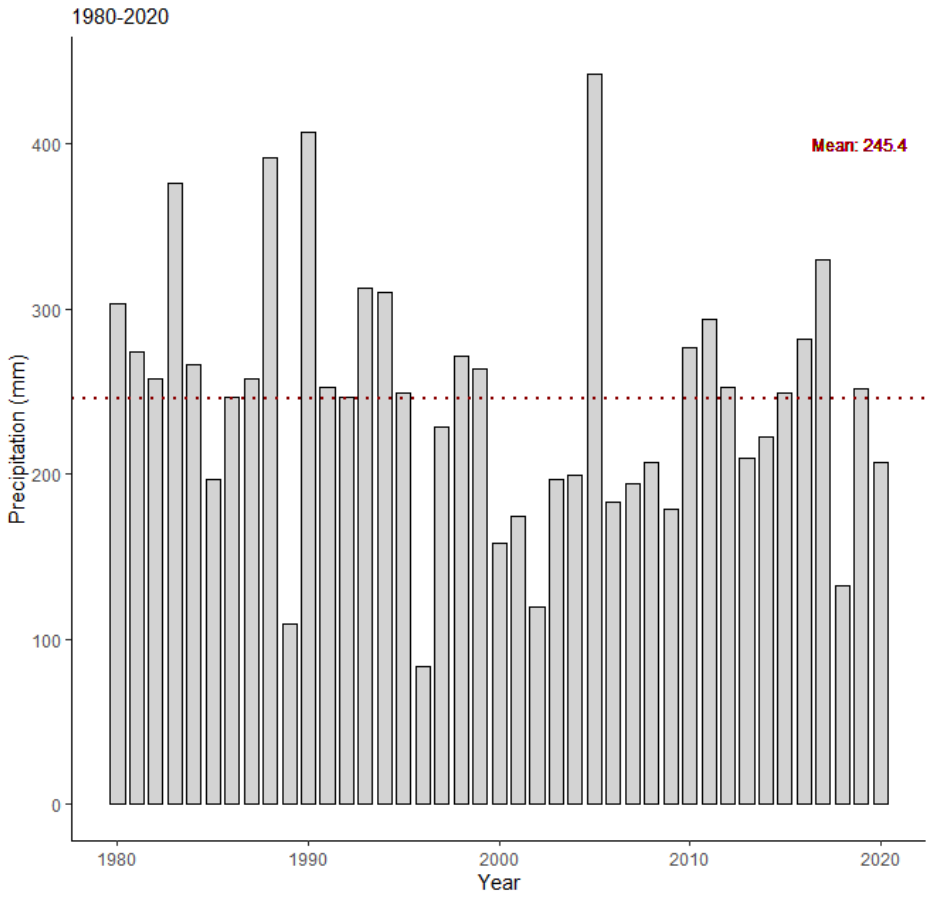

Figure 7 | Annual depth of precipitation for Peach Springs, AZ, using PRISM Climate Group Data from 1980-2020, with a mean annual 245.4 mm.

3.2.2. Classification of Dry, Normal, and Wet Years

The CV indicated high variability in annual precipitation, so a metric was needed to classify a normal year, a dry year, and a wet year to evaluate the difference in precipitation patterns and their annual potential effects on RWH. The Indian

Meteorological Department's specifications for classifying precipitation years was used to classify: a dry year as annual precipitation total that was less than the 23rd percentile or < 20% of long-term precipitation average; a normal year fell between the 23rd and 80th percentile or ± 20% of the long-term precipitation average; and a wet year was classified as any precipitation year that exceeded the 80th percentile or > 20% of long-term precipitation average (IMD, 2022; Garg et. al. 2021). A probability density function was created to validate the classification of precipitation years within the 41-year period.

3.3 Rainwater Harvesting (RWH) – Water Budget

The volume of water that could be captured from the rooftop of the four buildings was determined by modifying the following equation expressed by Aladenola et al, (2009) which was adapted from Ghisi et. al., (2006):

$$V_r = \frac{R_d \times A_r \times R_c}{1000} \qquad [3]$$

where V_r is the volume of rainfall that can be harvested (m^3), R_d is the rainfall depth (mm), A_r is the rooftop area (m^2) of the given buildings (see table 1), and R_c is the runoff coefficient determined by the rooftop material of said buildings (Anchan and Shiva, 2021).

3.4 Aqua Crop Model

For this study, the AquaCrop model was used to determine the net irrigation required for the yield of the following calibrated crops: maize, potatoes, tomatoes, and sunflowers— four crops already grown in the Hualapai Community Garden, as well as the dry yield that can be obtained during the growing season. The growing season runs from May to September, with some colder tolerant plants cultivated in April. There were three projects for each crop, with precipitation classified as a dry, normal, or wet year, for a total of 12 projects. Monthly inputs were used, based on availability from PRISM.

The ETo was calculated using the FAO's ETo Calculator— a software developed to determine the reference evapotranspiration according to the FAO's standards using the Penman-Monteith equation (FAO, 2022). The ETo Calculator has an extension option for the AquaCrop model, allowing the calculated ETo to be directly inputted into the desired project. Soil characteristics was inputted as fine sandy loam per observation and confirmed by the Natural Resources Conservation Service (NRCS) Soil Survey of Mohave County, Arizona (2005).

3.5 Climate Projections

Climate projections for precipitation as well as minimum and maximum temperature were plotted into a time series for water years 1950 to 2099 by Dr. Christine Albano. They were created in imperial units and analyzed as such. The plotted data represent a view into possible future climate for the area to determine the future feasibility of RWH. Climate projections for the area were developed using 15 global climate models (GCMs) from the Climate Model Intercomparison Project, Phase 5

(CMIP5). CMIP5 is the standard framework focused on the understanding and comparison of multiple GCMs to improve the knowledge of the changing climate processes and feedbacks (Kamworapan et al., 2019; Sheffield et al., 2013). CMIP5 evaluates the how well GCMs simulate the recent past, provides future climate projects for two different time scales—near and long term (2035 or 2100, respectively), and attempts to understand the factors that are responsible for the different simulation outcomes (PCMDI, 2022)

The 15 CMIP5 GCMs represent the best projections for the western US compared to historical observations (Lynn et al., 2015). Two different scenarios were considered - representative concentration pathways or RCP 4.5 and RCP 8.5, which depict moderate and accelerating GHG, respectively. GCMs are statistically downscaled using the Local Constructed-Analogs (LOCA) method, which estimates the effects of topography on local weather patterns by downscaling to the 1/16th degree, or 6 km (Pierce and Cayan, 2014). Further information on the GCMs used for CMIP5 in the region can be found in California Department of Water Resources' Perspective and Guidance for Climate Change Analysis (Lynn et al., 2015).

4.0 Results and Discussion

The four buildings considered for RWH on the Hualapai Reservation are shown in Figure 8 and summarized in Table 1. The 4H building has a galvanized roof (0.9 R_c) and a 4:12 pitch, meaning the roof rises 4 in (10.2 cm) every 12 in (30.5 cm). The roof of the 4H building is approximately 278 m^2 with 15.2 cm gutters and 10.2 cm by 12.7 cm downspouts. The three other buildings (greenhouse, tractor and tool shed) are in the Hualapai Community Garden. The roof materials of each building, R_c and individual roof area are listed in Table 1 The combined roof area for the 3 buildings is approximately 79.4 m^2.

Table 1 | Characteristics of the four buildings considered for RWH

Building	Roof Material	R_c	Area (m^2)	Roof Pitch (Slope)
4H	Galvanized Metal	0.9	278	35°
Tractor Shed*	Asphalt Shingles	0.7	55.7	35°
Tool Shed*	Asphalt Shingles	0.7	17.8	35°
Greenhouse*	Plexiglass/Wood	0.8	5.9	40°

* Three buildings were combined since they are in the same area—community garden. Combined area is 79.4 m^2.

Figure 8 | | (a) 4H building considered for rainwater harvesting on the Hualapai Reservation consist of a galvanized metal roof and approximately 278 m^2. (b) Additional buildings considered for rainwater harvesting in the Hualapai Community Garden with a combined roof area of 79.4 m^2.

4.1 Climate Characteristics

Precipitation

Summary statistics of annual and monthly precipitation patterns are listed in Table 2. A decrease from 279 mm (reported in existing literature) to approximately 245 mm is noted. Most literature reports precipitation until 2005, slightly after the start of the ongoing drought, which might be responsible for the higher precipitation values. Additionally, the 279 mm is based on station observation while the PRISM data is based on statistical methods used to interpolate and represent a 4km scale, rather than a single point. The standard deviation among years is 77.3 mm, suggesting a large variation in precipitation pattern. The interannual coefficient of variation is 0.32, suggesting high variability in precipitation between years. Additionally, it suggests that precipitation will vary ± 32% from the long-term average approximately 68% of the time, based off the empirical rule for standard deviation. The skewness for annual precipitation is 0.34, making it rightly skewed, suggesting that a few precipitation values are pulling the mean further right, making it greater.

Statistical parameters for monthly precipitation (Table 2) over the four decades show greater variability in all months relative to annual precipitation. Maximum average precipitation is observed in the monsoonal months of July and August, having a standard deviation less than their corresponding mean values. Greater variability in precipitation is also observed for the winter months of December, January, and February. The remaining months show a lower mean than their corresponding standard deviation, which indicates

a larger variation in the distribution of precipitation over the months. This suggests that the months of the summer monsoon and the winter months have slightly more reliable precipitation patterns that cluster around the mean than other months. Arizona receives some of its precipitation during the winter and most during the summer monsoon. Coefficient of skewness for all months is positive with most numbers closer to one and all numbers < 2. The positivity of skewness indicates that the data are skewed to the right from the normal distribution. The positively skewed months of precipitation show that monthly mean for that specific month is greater than the monthly median.

Table 2 | Summary statistics for annual and monthly precipitation 1980-2020

Month	Mean (mm)	Standard Deviation (mm)	Coefficient of Variation	Coefficient of Skewness
January	22.6	21.8	0.96	0.84
February	29.7	26.5	0.89	1.65
March	22.3	20.4	0.91	1.01
April	12.1	13.5	1.12	1.90
May	7.2	10.0	1.39	1.78
June	4.9	7.1	1.44	1.93
July	31.0	27.4	0.88	1.52
August	36.3	21.9	0.60	0.77
September	22.4	19.5	0.87	0.84
October	14.9	16.5	1.11	1.30
November	16.6	20.6	1.24	1.81
December	25.5	22.4	0.88	0.72
Annual	245.0	77.3	0.32	0.34

Peach Springs receives most of its precipitation during the monsoonal months of July-September and the cooler months from December- February as seen in Figure 9 from 1980-2020 data. The box and whisker plot for mean monthly precipitation show a

vast variability in precipitation amounts for each month, with great variability during the monsoonal months and the winter months. With most of the annual precipitation falling during the growing season, the potential for RWH increases, since the water captured can be applied directly to the irrigation system. Although water can be captured during the winter months, additionally cost are accrued since further engineering and storage is needed. For this study, we will be focusing on rainwater harvesting feasibility for the growing season in Peach Springs from April/May- September.

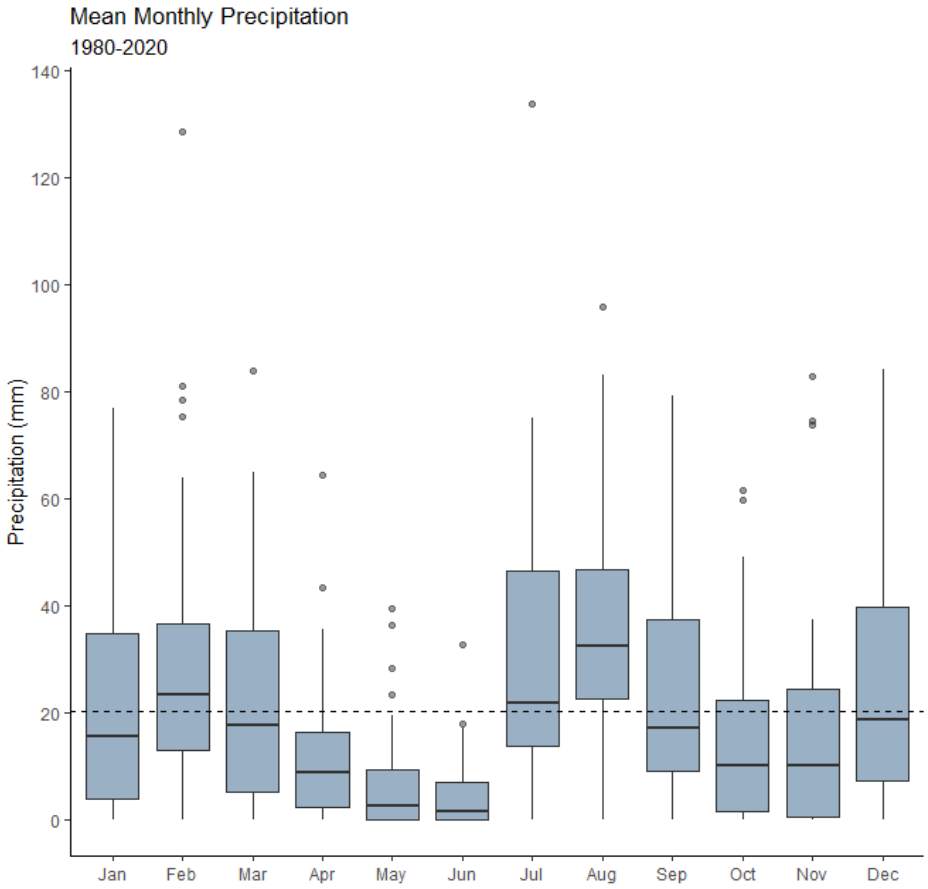

Figure 9 | Mean monthly precipitation of Peach Springs with an overall monthly mean of 20.5 mm. Most precipitation occurs during the summer months of July-September and winter months December- February.

The decomposition time series separated the seasonal, trend, and noise from the dataset. The trend (Tt) component is seen in Figure 10 with a LOWESS smoothing (blue) with a 1/10 smoothing span —the complete decomposition figure can be found in the Appendix (8.1). The isolated LOWESS smoothing is shown for mean monthly precipitation in Figure 11a and b, with smoothing span 1/10 and 2/3, respectively. The smoothing span controls the amount of "smoothness" of a series.

Figure 11a, shows monthly precipitation from 1980-2020. During the 1980s until the early 1990s, mean monthly precipitation values appear to increase and decrease around 20 mm mark. In the 1990s, the entire curve shifts downward, increasing and decreasing around a lower mean value. Figure 11b shows the mean monthly precipitation data with a LOWESS smoothing span of 2/3 (blue). Monsoonal seasonality, or noise, is removed at a greater degree. The smoothing shows a general trend of the mean monthly

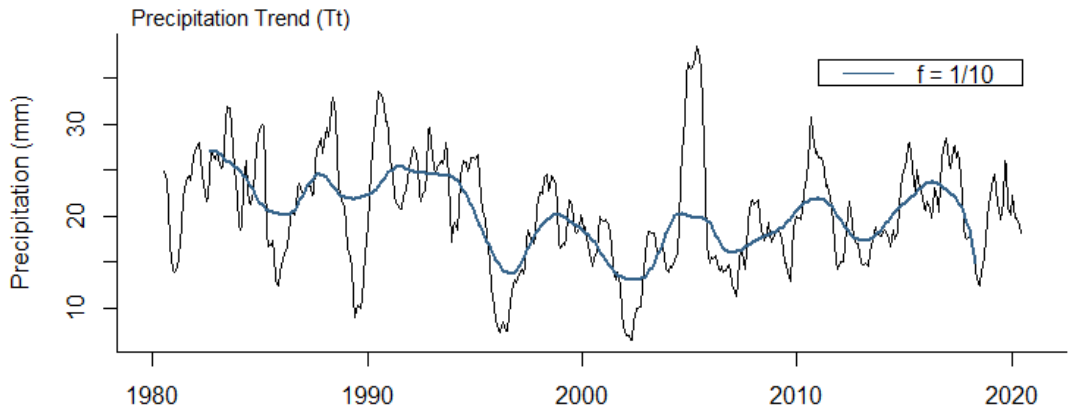

Figure 10 | Precipitation trend (Tt) as shown in the decomposition of time series. LOWESS (blue) with a smoothing span of 1/10th (0.1) shows a downward trend in mean monthly precipitation. Full decomposition figure can be found in the Appendix (8.2).

precipitation decreasing from 1980 until the late 2000s, with a minor increase in the early 2010s, followed by a gradual leveling off. Note that the LOWESS smoothing with a span of 2/3 smooths the series more aggressively than the moving average.

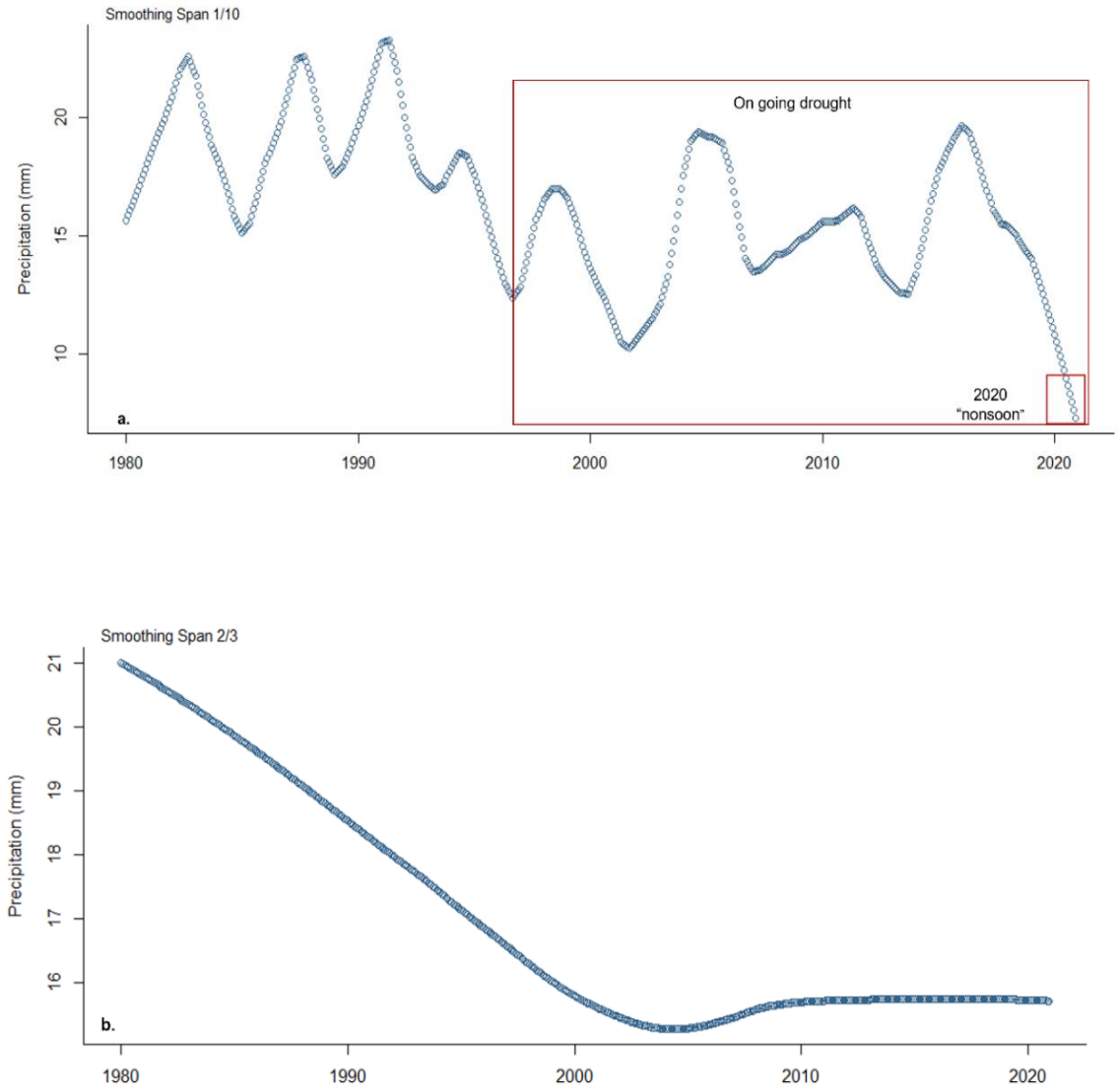

Figure 11 | (a) LOWESS smoothing with a span of 1/10 on the raw monthly precipitation timeseries. Outline (red) is the ongoing drought in the Southwest and the steep decline in precipitation during the 2020 "nonsoon". (b) LOWESS smoothing with a 2/3 smoothing span shows the generalized, or significantly smoothed, mean monthly precipitation. Precipitation seems to level out after the 2010. Mean monthly precipitation has decreased from approximately

The decrease in monthly precipitation coincides with the drought ongoing in the Southwest since the late 1990s. This drought has also been affecting the larger Colorado River Basin. Though there are some peaks of precipitation in the mid-2000s and 2010s, but there appears to be no sustained recovery to 1980s levels. Additionally, the 2020 monsoon, which was coined “the nonsoon” for its nonexistent precipitation during the monsoon season as well as the winter months (Leonard, 2021), shows smoothed monthly precipitation falling below 5 mm. This is the lowest precipitation for the data set, which has contributed to the decrease in the overall mean monthly precipitation for the study area.

Temperature

Summary statistics for annual and monthly temperature between 1980 and 2020 are shown in Table 3. The interannual coefficient of variation for annual temperature is 0.05, indicating that variability is less evident in the temperature data. Standard deviation between years is also relatively low at 0.7, suggesting that there is less variability of the annual mean temperature from year to year. The skewness represents the distribution of data about the mean. For annual temperature data, the positive skewness at 0.24 indicates data skewed to the right on a normal distribution curve. This value suggests that a few temperature values pull the mean to the right of the median, creating slightly greater variability.

The summer months June, July, August, and September, have the maximum average temperatures and the minimum temperatures during the winter months, December-February (Figure 12). As summarized in Table 3, standard deviation for mean

monthly temperatures are low, the coefficient of variation is also low suggesting that the data is more consistent. Coefficient of skewness is negatively or positively skewed depending on the month. The data set is approximately symmetric.

Table 3 | Summary statistics for annual and monthly temperature 1980-2020

Month	Mean (°C)	Standard Deviation (°C)	Coefficient of Variation	Coefficient of Skewness
January	5.0	1.7	0.34	0.52
February	5.8	1.8	0.30	0.09
March	8.4	1.6	0.19	0.16
April	12.0	1.7	0.14	0.00
May	16.8	2.0	0.12	-0.10
June	22.4	1.6	0.07	-0.49
July	25.4	1.0	0.04	-0.28
August	24.6	1.1	0.04	0.58
September	21.1	1.3	0.06	-0.57
October	14.9	1.6	0.11	0.33
November	8.9	2.0	0.22	-0.27
December	4.8	1.6	0.32	0.23
Annual	14.2	0.7	0.05	0.24

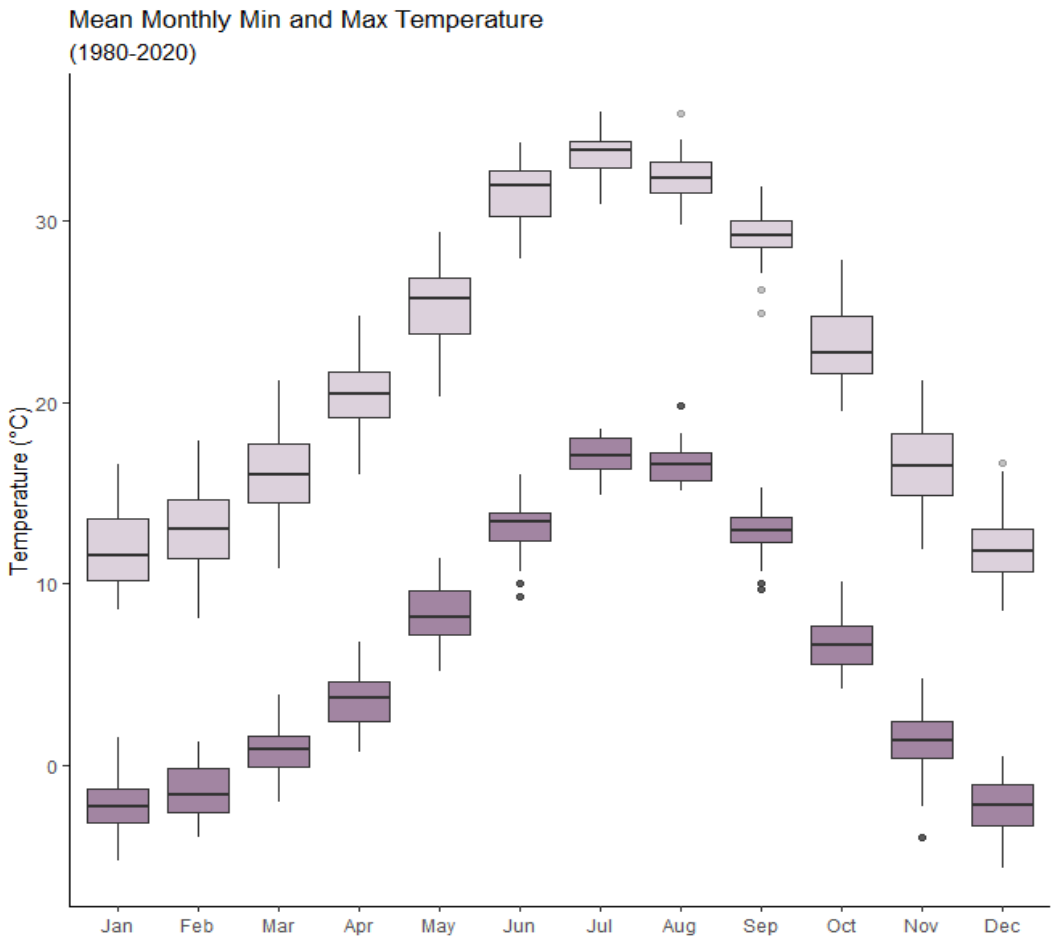

Figure 12 | Mean monthly minimum and maximum temperature of Peach Springs (1980-2020). Highest temperatures occur during June- September and the cooler months occurring during December to January.

The decomposition time series for temperature shows the trend (Tt) component (Figure 13) with monthly temperature from 1980 to 2020 with a LOWESS smoothing line with a 1/10 smoothing span in purple. The high temperatures from 2000 to 2020 coincide with the ongoing drought in the Southwest, classified as the warmest and driest period on record and 2020 was determined to be extremely arid (Williams et al., 2022). Figure 14a shows high temperature and aridity observed in the study area. The data

suggests an increase in mean monthly temperature from ~ 13.5 °C to 15.0 °C (Figure 14b) during 1980 to 2020.

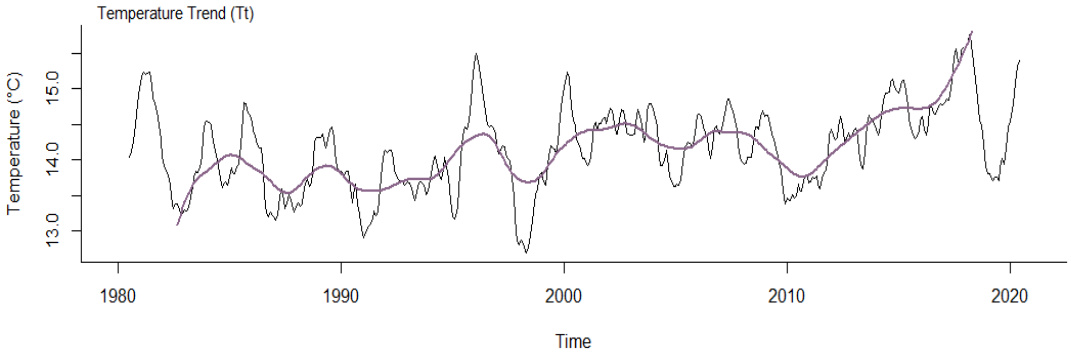

Figure 13 | Temperature trend (TTt) as shown in the decomposition of time series. LOWESS (purple) with a smoothing span of 1/10th (0.1) shows an upward trend in mean monthly temperature.

The warmest months coincide with the wettest months during the year, suggesting that evaporation and ET are high. Hourly precipitation for 2019 was evaluated in a separate exercise using the HYDRUS-1D model to determine if rainfall would create enough runoff for in-field RWH (the collection and concentration of rainfall via conduits and furrows in the ground to desired agricultural area, see Figure 3). Although it was determined to not be feasible, rooftop RWH was possible when hydraulic conductivity was reduced to zero (equivalent to the infiltration of a metal roof). This shows that rainfall can still be collected with maximum temperatures present during the wet summer months.

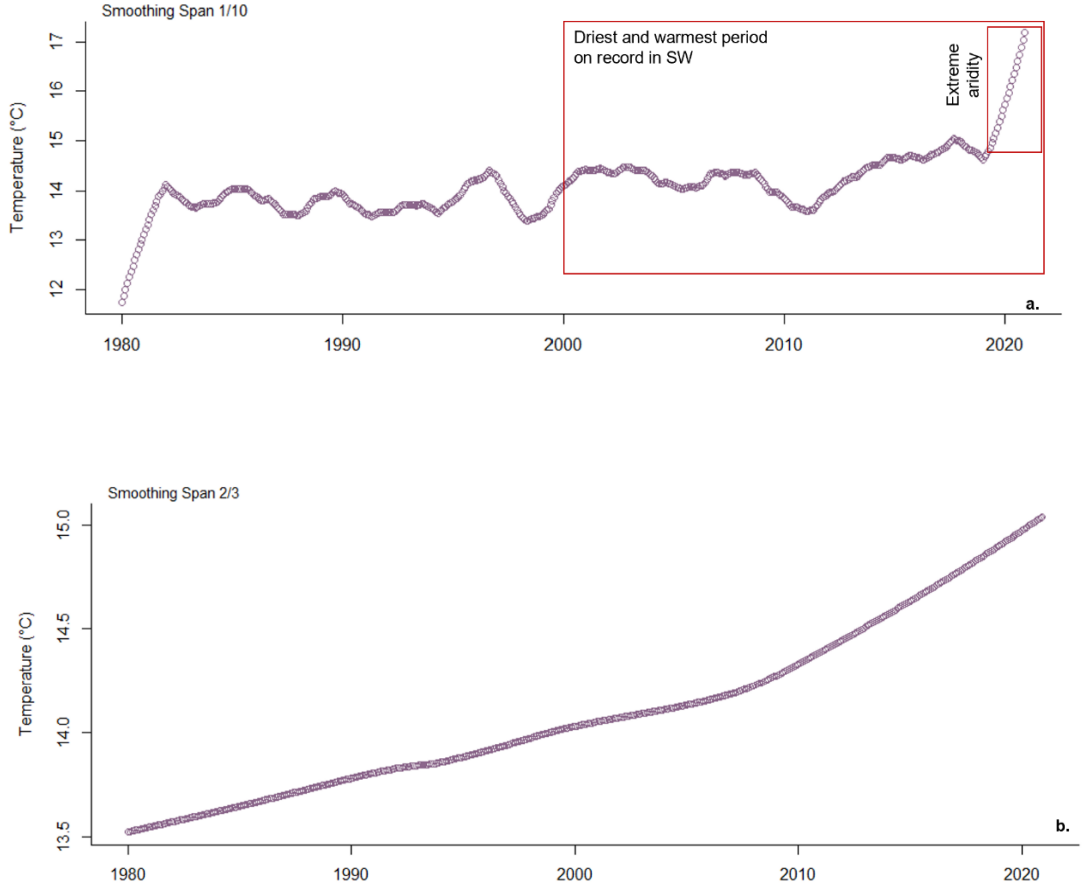

Figure 14 | (a) Isolated LOWESS smoothing with a span of 1/10 of mean monthly temperature for Peach Springs, AZ. Outlined in red highlights the driest and warmest period on record since 800 A.D. as stated by Williams et al. (2022). The year 2020 was classified as being extremely arid in the Southwest (SW) along with the year 2021 which was excluded from this study. (b) LOWESS smoothing with a 2/3 smoothing span shows the generalized, or significantly smoothed, mean monthly temperature. Note: LOWESS smoothing with a 2/3 span is more aggressive than the moving average.

Classification of Normal, Dry, and Wet Precipitation Years

The CVs indicate high variability in precipitation, so years were classified as normal, dry, and wet precipitation years according to the Indian Meteorological Department's specifications (described in methods section). The precipitation amounts were categorized by water years. Table 4 shows summary statistics for these classifications. A normal year was classified as any annual precipitation between 196 mm -294 mm or within the 23rd-80th percentile with an average precipitation of 244 and a standard deviation of 28.4 mm. A dry year was classified as any value 20% less than long-term average or less than 194 mm, falling below the 23rd percentile. Average precipitation for a dry year is 148 mm with a standard deviation of 36.3 mm. Lastly, a wet year was classified as annual precipitation greater than 290 mm or greater than the 80th percentile. Average precipitation for a wet year was 359 mm with a standard deviation of 48.9 mm. A probability density function was created to validate the classification of precipitation years within the time frame (Figure 15).

Table 4 | Classification for precipitation in Peach Springs, AZ from 1980-2020

		Percentile (%)	*n*	Average Precipitation (mm)	Standard Deviation (mm)
Normal	194-290 mm	23-80%	24	244	28.4
Dry	<194 mm	<23%	9	148	36.3
Wet	>290 mm	>80%	8	359	48.9

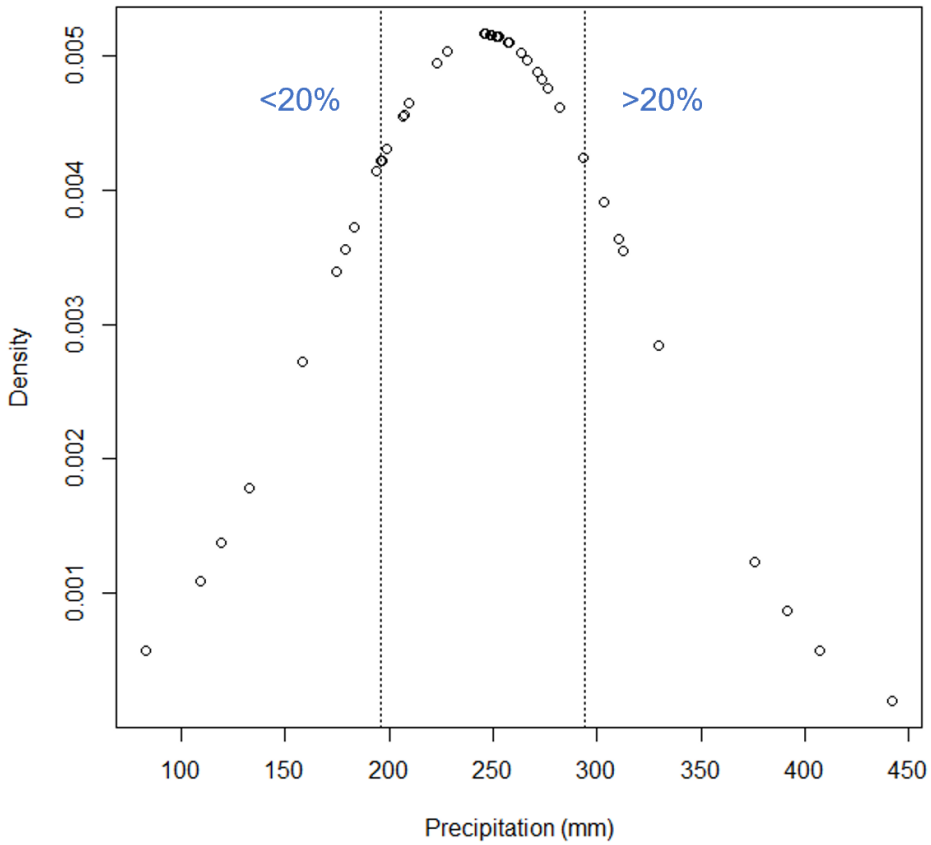

Figure 15 | Probability density function of annual precipitation for Peach Springs, AZ from 1980 to 2020 water years. The Indian Meteorological Department guidelines for classifying a normal, wet, and dry precipitation year was used which indicates that any values less than 20% of the long-term precipitation average is considered a dry year, more than 20% of the long-term average is a wet year and anything in-between is considered normal. The dashed vertical lines indicate the ±20% from the long-term average, the cluster of data falls within the limits.

Monthly precipitation averages for a normal, dry, and wet year are shown in Table 5 and in box plots on Figure 16. The median values (50^{th} percentile) for August are slightly lower for the wet year than the corresponding normal year. The data suggest that during a wet year, more rainfall is received during the combined winter months of December, January, and February, than during the summer monsoon months of July, August, and September. A normal and dry year both receive most of the precipitation during the monsoon months of July, August, and September. This observation is significant since the collected rainwater would be used during the growing season of May -September.

Table 5 | Average Monthly Precipitation for a Normal, Wet and Dry year

Month	Normal Precipitation Year (mm)	Dry Precipitation Year (mm)	Wet Precipitation Year (mm)
January	19.1	13.4	43.4
February	27.8	15.8	52.1
March	24.7	13.2	25.3
April	11.7	4.2	22.2
May	8.9	1.3	8.7
June	4.0	3.7	9.1
July	30.9	25.2	37.7
August	36.1	30.1	43.7
September	25.9	13.8	21.5
October	12.8	12.1	24.3
November	17.4	4.3	28.4
December	25.1	11.2	42.7

Regardless, a wet year receives the greatest precipitation during both the winter and the summer months as compared to a normal and dry year. For each year, most precipitation occurs during the month of August for a normal and dry year, while a winter year receives the greatest precipitation amounts during February at an average of 52.1 mm. The lowest precipitation amounts occurring during May for a wet and dry year, while a normal year receives the least amount of precipitation during the month of June. This

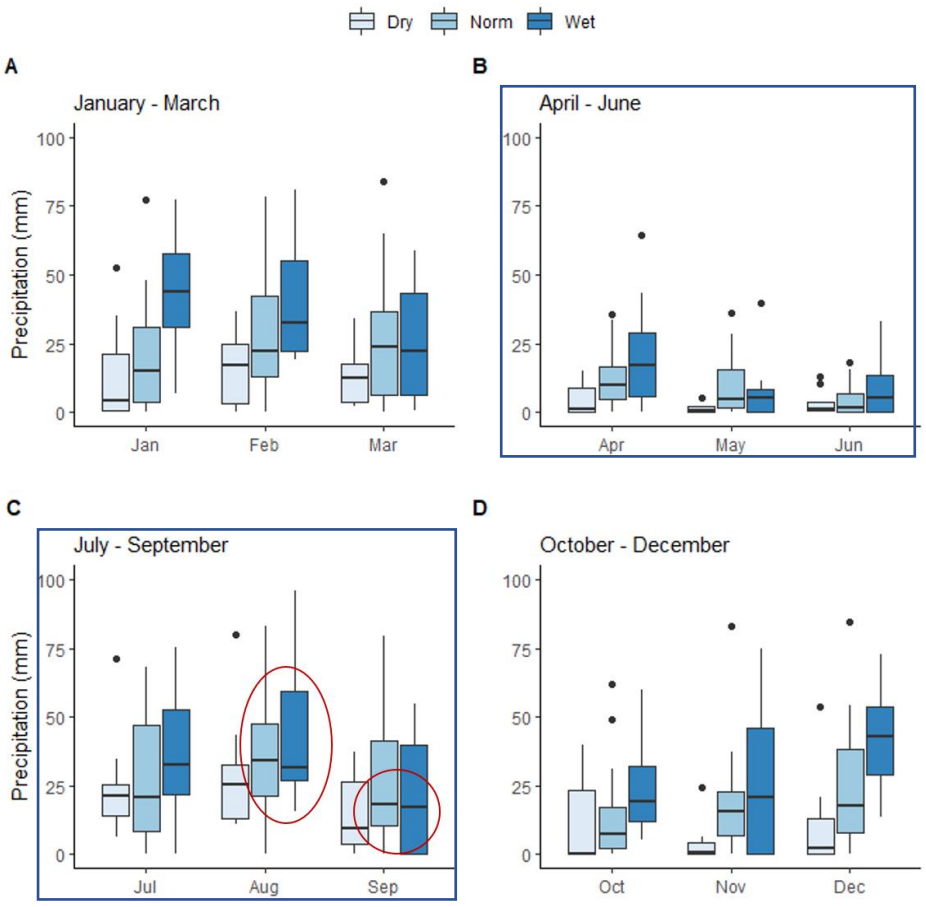

Figure 16 | Average monthly precipitation depths in Peach Springs during a dry, normal, and wet year. The summer months of August in plot C, show a slightly higher median for precipitation during the classified normal year than a wet year. The month of September shows similar median values for both a wet and normal year. Cultivable areas in this study will focus on the precipitation amounts during the growing season for Peach Springs, April-September (blue boxes).

coincides with May and June being the driest months for the state Arizona, before the start of the summer monsoon (DeMeo, 1991). The data suggest that variability is greater during the summer months for any given year as compared with other months. This finding agrees with Tamaddun et al., (2018) who studied precipitation patterns for the potential of RWH and observed higher variations during the summer months in the state of Arizona. When considering extremes, a wet August could have 17% to 32% more rainfall than a normal and dry monsoonal month, respectively. A wet February month could have as high as 47% to 70% more rainfall than a normal and dry February, respectively.

4.2 Rainwater Harvesting

4H Building

The catchment area of the 4H building is approximately 278 m^2 with a runoff coefficient of 0.9. The average volumes of rainwater that can be potentially collected per month during a normal, dry, and wet year, using equation [3], are listed in Table 6. There are some interesting differences between volumes that can be captured during all the months of normal, dry, and wet years. During the winter months of December, January, and February, approximately 42% more volume can be collected during a wet year than a normal year and 81% more than a dry year. During the monsoonal months of July, August and September, a wet year can generate approximately 25% more volume than a normal year and 44% more than a dry year. August seems to produce the highest volume for every classified year for the summer monsoonal months.

Table 6 | Average volume of potential harvestable rainwater during classified years for the 4H building

Month	Normal Year (L)	Dry Year (L)	Wet Year (L)
January	4,758	3,350	10,813
February	6,918	3,927	12,988
March	6,152	3,289	6,308
April	2,910	1,051	5,543
May	2,231	315	2,166
June	998	911	2,261
July	7,699	6,280	9,405
August	9,003	7,504	10,904
September	6,449	3,438	5,357
October	3,200	3,012	6,051
November	4,328	1,070	7,071
December	6,257	2,784	10,645
Annual	60,903	36,931	89,512
Growing Season	**29,289**	**19,499**	**35,637**

The highest volume that can be collected is 12,988 liters from the 4H building during a wet year in the month of February. The lowest overall volume is 315 liters during May of a dry year. Figure 17 shows the average volumes of rainfall that can be collected from the 4H building per combined months during a water year. The months were combined to better display the amounts of collatable water. Plot A accounts for the first three months of a water year, October, November, and December. Plot B accounts January, February, and March. Plot C accounts for the months of April, May, and June and while D accounts for the summer monsoonal months of July, August, and September. The cooler (B) and warmer months (D) see the highest precipitation amounts, allowing

for more water to be collected during that time. During time D of both a normal and wet year similar volumes can be collected.

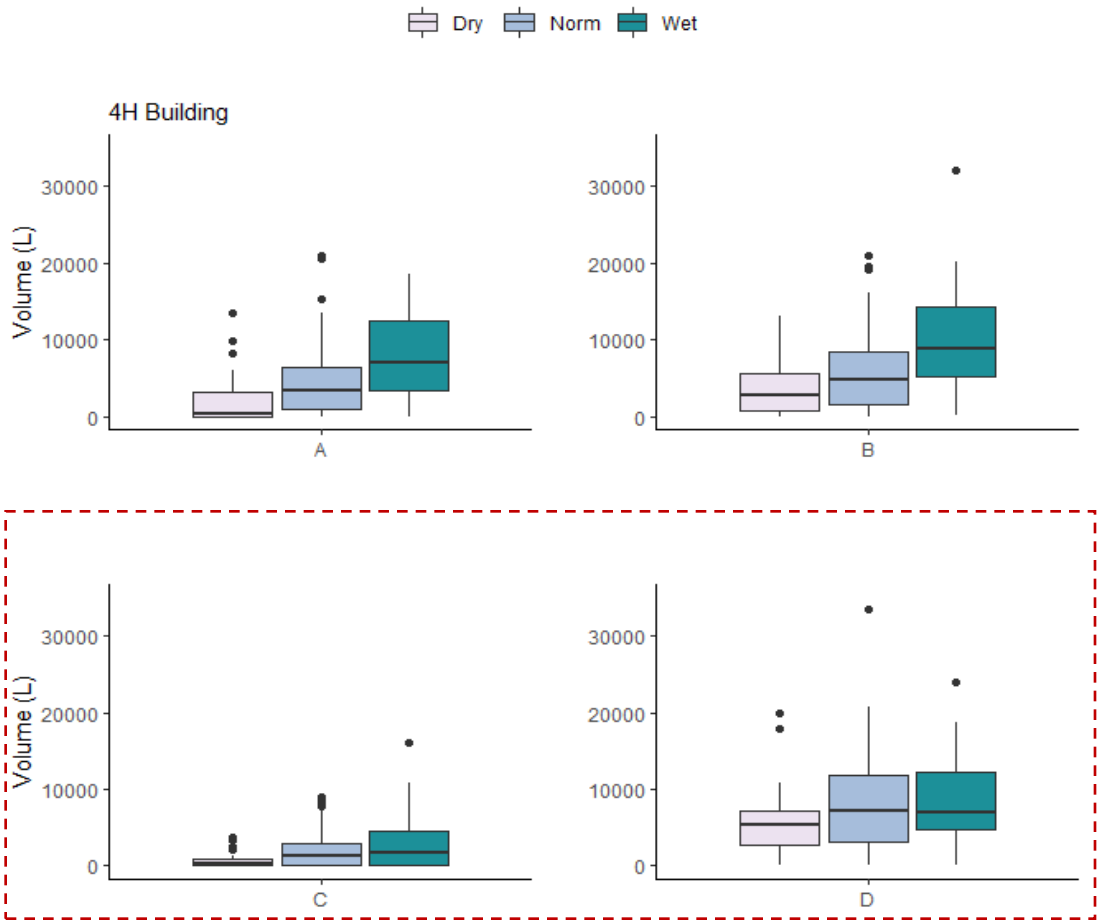

Figure 17 | Volume (L) of rainwater that can be collected during a dry, normal, and wet year during for the 4H building. Oct-Dec (A), Jan-Mar (B), Apr-Jun (C), Jul-Aug (D). Both C and D represent the growing season which will be the focus of the cultivation (red dash line).

During the growing season, April-September, a total of 29,289 liters of rainwater can be collected from the 4H building during a normal precipitation year and 19,499 liters and 35,637 liters, can be collected during a dry and wet year, respectively. The water collected from the 4H building during the growing season would help irrigate a

garden to be used for food production. The plot of land considered for cultivation is shown in Figure 18. Using Google Earth, the area is determined to be approximately 150 m^2. Rainwater harvesting can also be practiced during the rest of the year, for instance, the month of February can provide an abundance of collectable rainwater, however, due to the cooler minimum temperatures in Peach Springs averaging 5.8 °C, additional engineering will be needed to keep the water from freezing within the cistern. Burial or insulation of the cistern is required. Furthermore, since water is not being used until the start of the growing season, the volumes of the cisterns will need to increase to assure the full potential of rainwater harvesting for the entire year. These additional suggestions will increase the cost of the RWH project. This study focuses on the water that can be collected during the growing season for food production. Therefore, rainwater harvesting will be focused on the months of April through September, which is the growing season for Peach Springs.

Figure 18 | Prospective area for additional community garden behind the 4H building. Harvested rainwater would be used to help supplement the water needed for irrigation. Approximate area: 150 m².

Hualapai Community Garden

The three buildings considered for RWH in the Hualapai Community Garden - tractor shed, tool shed and greenhouse- have a combined catchment of 79.4 m^2 with an average runoff coefficient of 0.73. The patterns of volumes that can be collected are similar to those of the 4H building. The highest volume that the Community Garden buildings can collect is 3,020 liters during February in a wet year. The lowest amount that can be collected is 73 liters during May in a dry year. The collected volume during the growing season would help irrigate the existing crops in the Community Garden as seen in Figure 19; the area of the garden is approximately 320 m^2. Figure 20 shows average volume from the Community Garden buildings. Like the 4H building, higher volumes can be collected during the cooler months (B) and warmer months (D) for all classified years. The months April-Jun and Oct-Dec produce the least volumes for all years. During the growing season a total average of 6,810 liters can be collected from the three buildings and, 4,534 and 8,286 liters during a dry and wet year, respectively.

Table 7 | Average volume of potential harvestable rainwater during classified years for the Community Garden buildings

Month	Normal Year (L)	Dry Year (L)	Wet Year (L)
January	1,106	779	2,514
February	1,609	913	3,020
March	1,430	765	1,467
April	676	244	1,289
May	519	73	504
June	232	212	526
July	1,790	1,460	2,187
August	2,093	1,745	2,535
September	1,500	799	1,246
October	744	700	1,407
November	1,006	249	1,644
December	1,455	647	2,475
Annual	14,160	8,586	20,812
Growing Season	**6,810**	**4,534**	**8,286**

Figure 19 | The Hualapai Community Garden provides provisions for the tribal members. The garden is managed by FRTEP agent, Elisabeth Alden. Approximate area of the garden in 320 m² (a) Stalks of Hopi Corn, a cultural staple in the Southwest. (b) Southern view of the garden. (c) Tomatoes vines growing in the garden.

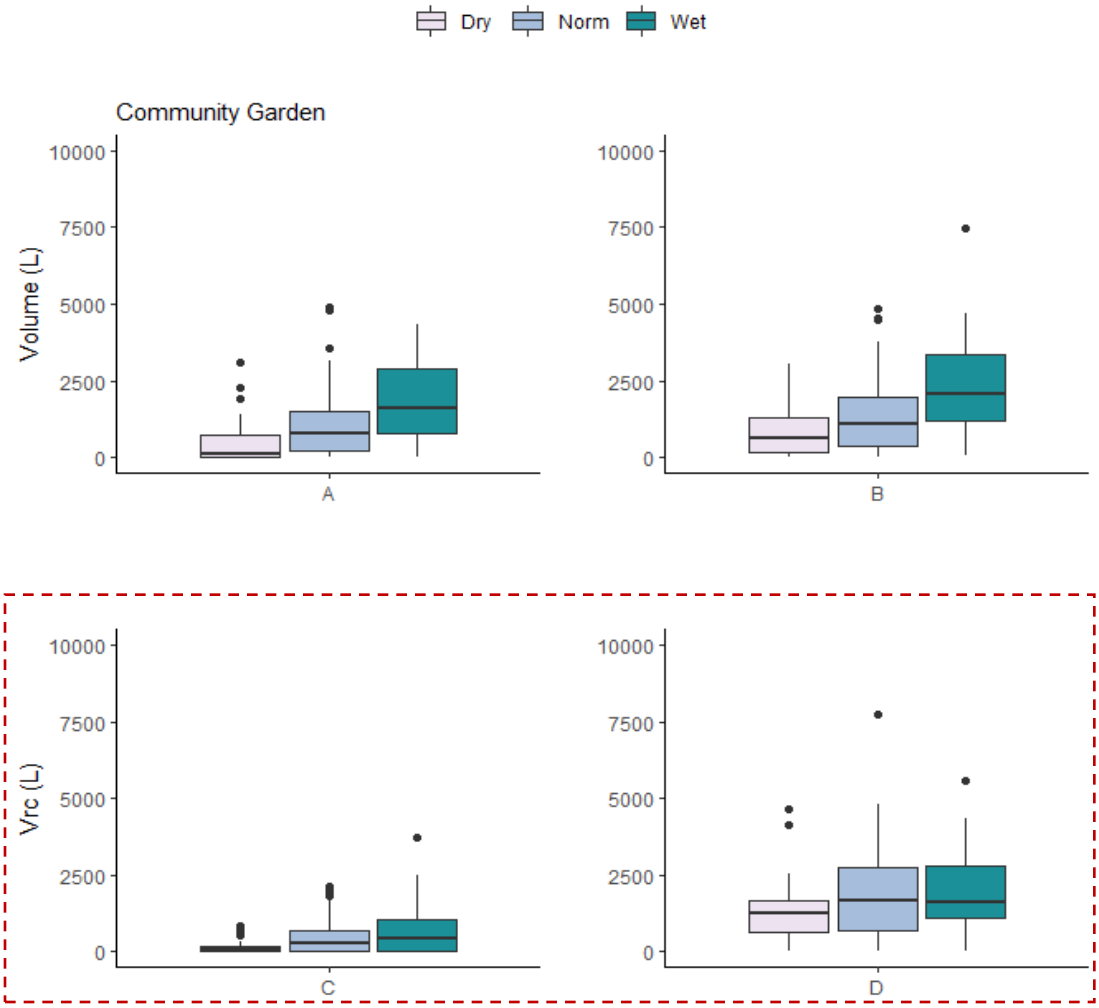

Figure 20 | Volume (L) of rainwater that can be collected during a dry, normal, and wet year from the Community Garden buildings. Oct-Dec (A), Jan-Mar (B), Apr-Jun (C), Jul-Aug (D). Both C and D represent the growing season which will be the focus of the cultivation (red dash line).

4.3 AquaCrop Model

The AquaCrop model was run for each crop for the three classified precipitation years— normal, dry, and wet, a total of 12 projects, for the growing season in Peach Springs, May-September, for the warmer tolerant plants. The month of April was considered for the rainwater harvesting and a part of the growing season, but not the planting period since all of the simulated crops are warmer crops sowed in the month of May, however, there are cooler tolerant plants that are currently being grown in the Community Garden, but not considered in the AquaCrop model. Simulated ETo, rainfall, net irrigation, and the area that can be cultivated using the harvested rainfall for the 4H building and the buildings in the Community Garden are listed in Table 8. The net irrigation considers the rainfall during the growing period (May-September) and determines the existing required irrigation for a healthy crop.

As expected, a dry year requires more irrigation for each crop than the corresponding normal and wet year, since less rainfed irrigation is available. Rainfed irrigation is the direct precipitation falling onto crops. More area can be cultivated during a wet year solely using the harvested rainwater in addition to the rainfed irrigation. Table 8 also lists summary values for cultivable area of each crop. An average area of 55 m^2 of maize can be cultivated during a normal precipitation year while dry beans, tomatoes, and sunflowers can cultivate areas of 56 m^2, 65 m^2 and 59 m^2, respectively (see Figure 21). During a wet precipitation year, approximately 15% more area can be cultivated using the harvested rainfall than a normal year and about 50% more than a dry year.

Table 8 | Cultivatable area for different crops during a normal, dry and wet year within the growing season

Crop	Class. Year	Planting Period	Simulated ETo (mm)	Rainfall (mm)	Net Irrigation (mm)	4H Build. Volume (m^3)	4H Cultivatable Area (m^2)	CG Build. Volume (m^3)	CG Cultivatable Area (m^2)
Maize	Normal		683.4	106.6	529.8	29.3	55.3	6.80	12.8
	Dry	May-Sep	702.1	48.80	599.9	19.5	32.5	4.53	7.55
	Wet		685.9	94.90	539.4	35.6	66.0	8.28	15.4
Tomatoes	Normal		622.8	92.80	523.1	29.3	56.0	6.80	13.0
	Dry	May-Sep	638.6	43.80	580.8	19.5	33.6	4.53	7.80
	Wet		626.6	82.60	533.0	35.6	66.8	8.28	15.5
Dry Beans	Normal		582.9	87.00	453.2	29.3	64.7	6.80	15.0
	Dry	May-Sep	595.1	38.70	510.4	19.5	38.2	4.53	8.88
	Wet		587.1	78.10	463.2	35.6	76.9	8.28	17.9
Sunflowers	Normal		632.9	100.6	499.7	29.3	58.6	6.80	13.6
	Dry	May-Sep	648.7	46.30	564.1	19.5	34.6	4.53	8.03
	Wet		639.3	91.30	513.2	35.6	69.4	8.28	16.1

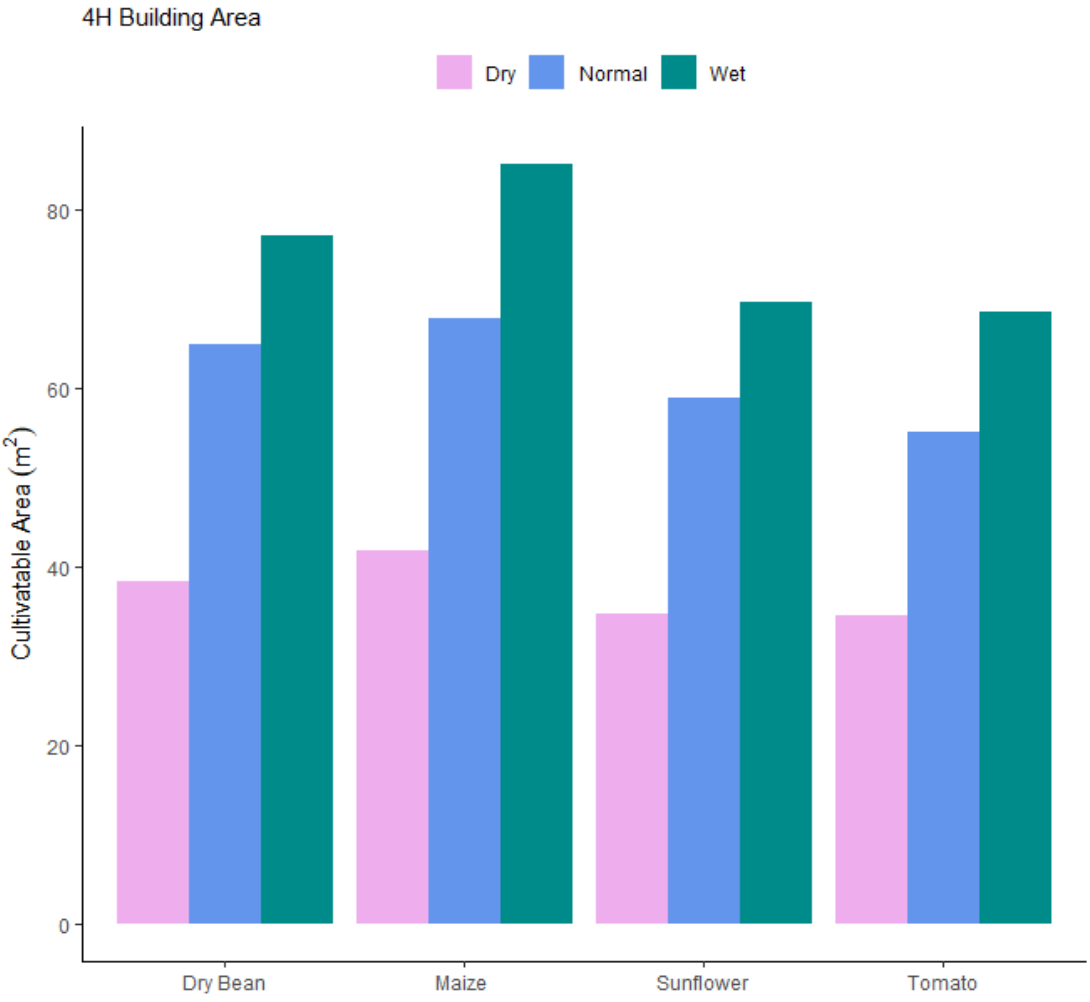

Figure 21| Area that can be cultivated by each crop during a classified precipitation year only using the harvested rainwater for irrigation from the 4H building.

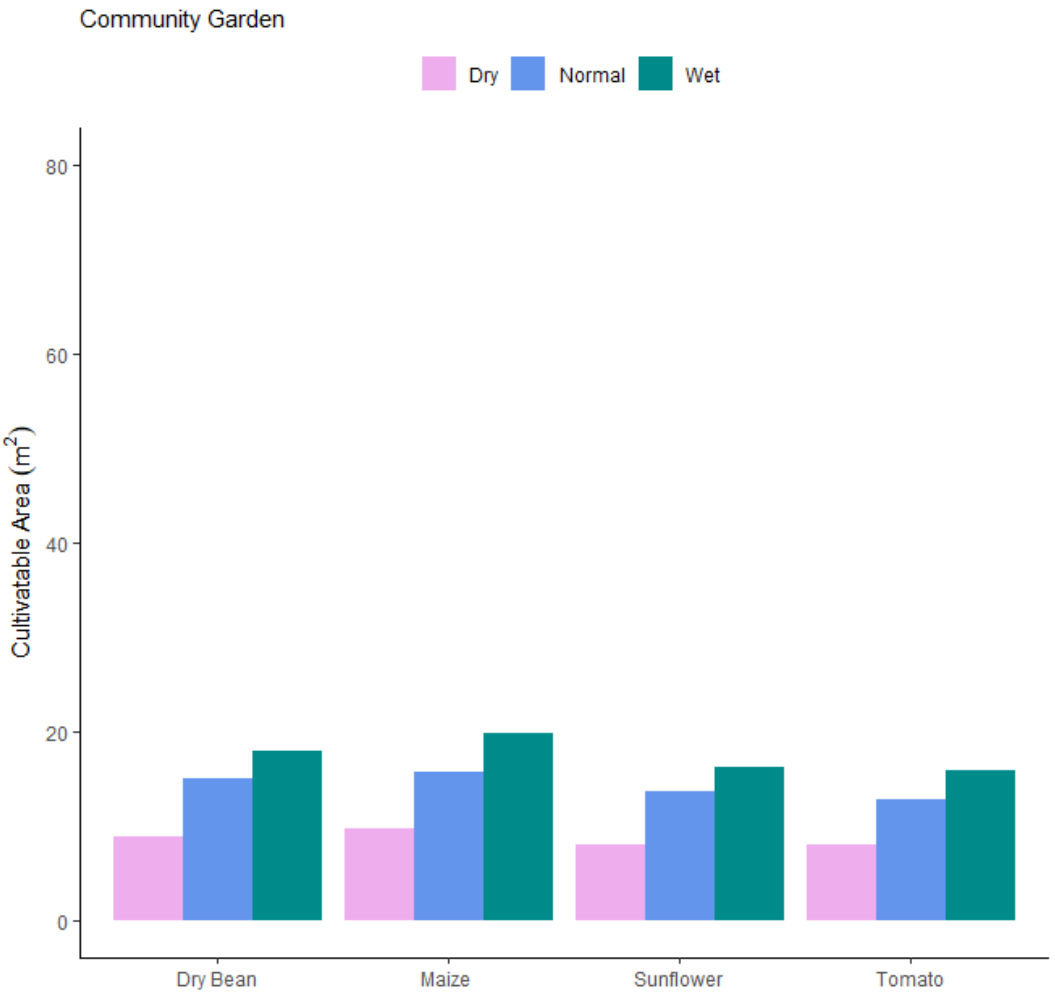

Figure 22 | Area that can be cultivated by each crop during a classified precipitation year only using the harvested rainwater for irrigation from the Community Garden buildings in addition to the rainfed irrigation considered in the AquaCrop model.

The area that can be cultivated for maize, dry beans, sunflowers, and tomatoes at the Community Garden is substantially less than the cultivable area at the 4H building as seen in Figure 22. The cultivable area for each crop is dependent on the amount of rainwater that can be captured during the growing season based on the catchment size. The catchment size of the 4H building is approximately 72% larger than the catchment area of the buildings in the Community Garden.

The average area that can be cultivated at the Community Garden is 14 m^2 during a normal precipitation year for any of the four crops. This is a small fraction of the existing garden (~4% or 1/20th of the area). Figure 23 shows a satellite image of the garden and the area that can be cultivated. Although the volume of water collected from the three buildings during the growing season (May-September) is relatively minimal in terms of providing irrigation for cultivating maize, tomatoes, dry beans and sunflowers, the alleviation of 4% of water used through current irrigation methods, can still be beneficial. The AquaCrop model also simulate the amount of crop yield that can be harvested at the end of the growing season for each crop. Looking at maize, the RWH and the rainfed irrigation for a normal precipitation year can generate a total of 18.3 kg

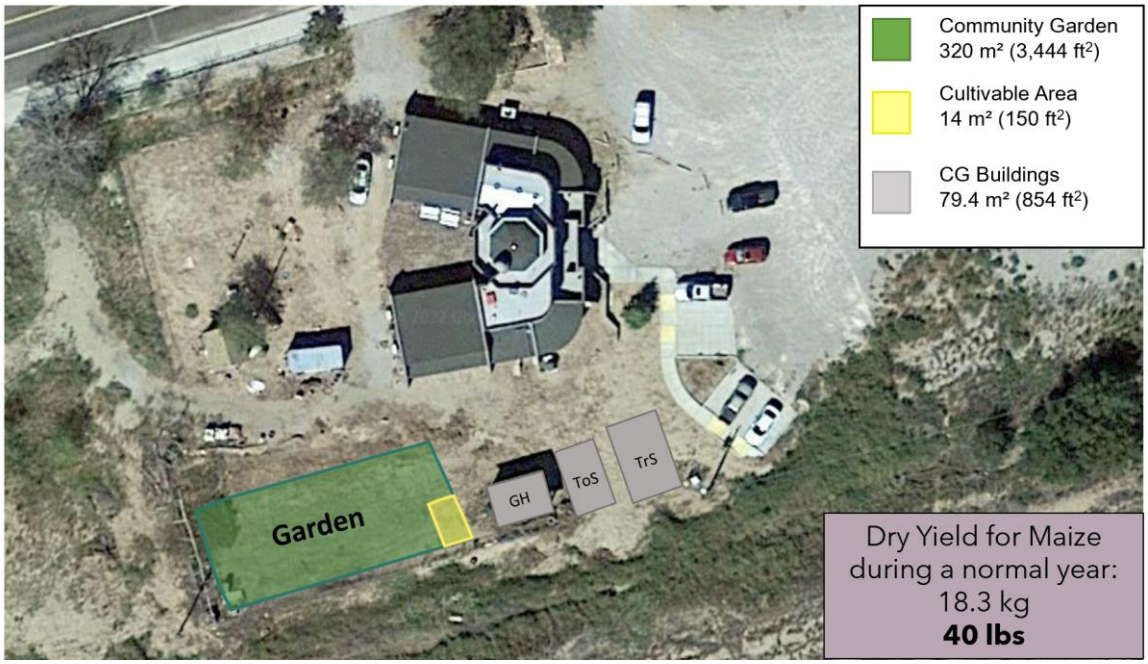

Figure 23 | Plan view of the Community Garden next to the Hualapai Cultural Center. The garden has an approximate area of 320 m^2 (green). The area that can be cultivated during a normal precipitation year is an average of 14 m^2 (yellow) and the area of the three buildings (greenhouse GH, toolshed ToS, and the tractor shed TrS) combined is 79.4 m^2. Source: Google Earth. AquaCrop determined that a total of 18.3 kg of maize can be harvested at the end of the growing season.

26% of the rainwater that could be collected during the growing season, so additional barrels would be needed to store the remaining rainwater.

Figure 24 | Existing rainwater harvesting material from a former project on the Hualapai Indian Reservation. (a.) Aluminum gutters that can be easily malleable to fit the roofs of the Community Garden buildings. (b.) Four rainwater harvesting cisterns that can hold 220 liters are also available.

The area that can be cultivated during the growing season using the volume from the 4H building is averaged at an area of 60 m^2 for a normal precipitation year. Figure 25 shows the plan view of the 4H building (blue), the prospective garden (green), and the area that could be cultivated (yellow). The volume during the growing season could help cultivate 40% or over 1/3rd of the prospective garden of 150 m^2 for an average of all crops. The AquaCrop model simulated a total of 81 kg (178 lb) of maize that can be

harvested at the end of the growing season during a normal precipitation year. Rainwater harvesting from the 4H building could help sustain a garden in the area for food production and sovereignty, at this scale.

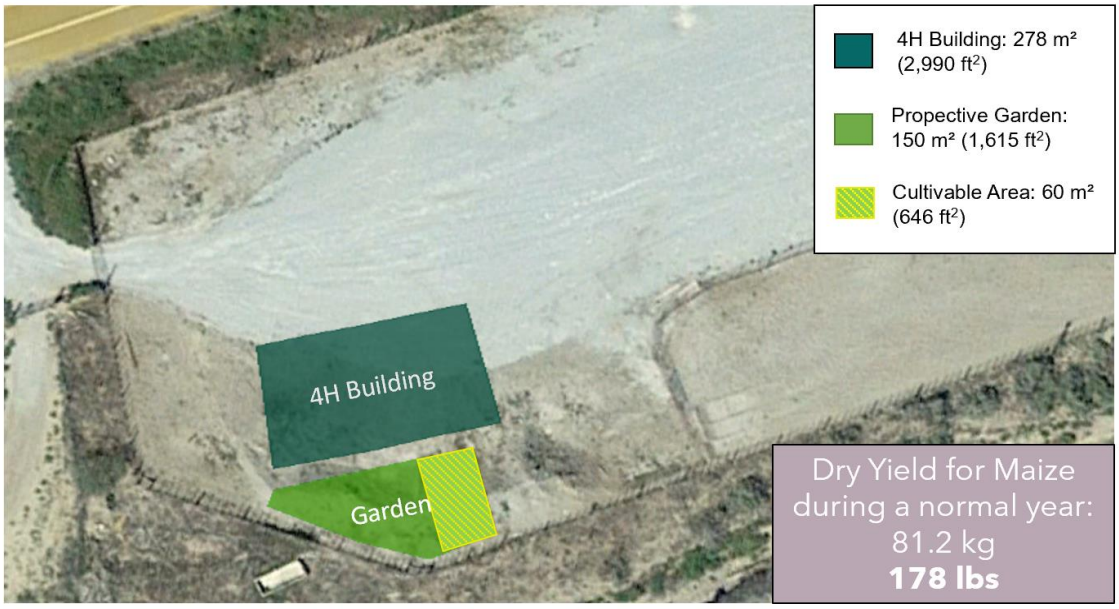

Figure 25 | Plan view of the 4H building (teal) with an area of 278 m2, the area of the prospective garden (green) with an approximate area of 150 m2 and the average cultivable area (62 m2) using the rainwater harvested from the 4H building (yellow). Source: Google Earth.

Cost of Materials

The average amount of water that can be collected during any classified year growing season (April-September) is approximately 6,543 liters for the Community Garden and 28,141 liters for the 4H building. Polyethylene/polypropylene rainwater cisterns are considered the most cost effective since they are durable, lightweight, come in a variety of sizes, and can be easily altered to inhibit the growth of algae for long term storage. These cisterns are commercially available with an average cost of $0.35 - $1.45 per 3.8 liters (1 gal) (TWDB, 2005). Prices were adjusted for inflation from 2005 to 2022.

The most effective size combinations for the 4H building would be either four 6,056-liter cisterns (1600 gal) to be installed in the four corners of the building, or two 18,927 liters (5000 gal) containers at two opposing corners. The Community Garden would benefit from an additional rainwater harvesting cistern that could hold at least 4,542 liters (1200 gal) to maximize the volume of water.

Additional items needed to implement RWH are cistern disinfectant, a pump, drip irrigation equipment, and a screen or strainer. A disinfection method is needed to assess the potential growth of algae and bacteria in the cisterns or tanks. Chlorine disinfection is a cost-effective method for non-potable outdoor water use. A pump or gravity can be used to allow for the effective release of water from the storage tanks to the crops or desired area. Drip irrigation is the most effective irrigation method which can “stretch” the water for cultivation since water is directly put on the plants root zone. A screen, strainer or filter will be needed to avoid clogging of the drip irrigation system (TWDB,

2005). Table 9 lists the estimated amounts for the necessary items and materials needed for RRWH for the Community Garden and the 4H building.

Table 9 | Estimated cost of basic RWH harvesting materials needed for 4H building and the Community Garden

Material	Average Cost (USD)	Size	Comments
Polyethylene/polypropylene Cisterns	$0.35 - $1.45 per 3.8 L (1 gal)	1,136 - 18,927 L (300-5,000 gal)	Size will be dependent on the landscape for RWH
Chlorine Disinfection (Calcium Hypochlorite)	$1.45 per month		Chlorine disinfection is the cost-effective method for non-potable outdoor use.
Leaf Screen and Strainer	$30-$50		Might not be needed since no foliage near the buildings
Small Water Pump	$435-$726		Pump or gravity will be useful to disperse water from tanks to crops
Drip Irrigation System	$0.48 per m^2	150 m^2 for 4H building 320 m^2 for CG	Drip irrigation is more effective, can help "stretch" the harvested water

Cost to Implement RHW in the 4H Building

During the growing season, the total cost to implement a rainwater harvesting system in the 4H building that would solely collect rainwater from April to September, would require cisterns, large enough to collect an average volume of 29,289 liters during

a normal precipitation year. A normal precipitation year is selected for the budget since it is the most common precipitation year in the 41-year record (1980-2020). The 4H building would require the most materials since it has a larger catchment size. The cost to implement a RWH system on the 4H building is listed in Table 10. At $0.35 to $1.45 per 3.8 liters or per a single gallon, polyethylene cisterns are the most cost effective. The cost of these containers would range from $2,697 - $11,175 to capture the average volume generated during the growing season. The gutter system already in place on the 4H building is suitable for a RWH system, therefore, there would be no additional cost. The pump is needed to deliver the water from the cistern to the garden and it is the most expensive component in an RWH system besides the cost of the cisterns. An average pump that can deliver water for irrigation costs an average of $435-$726. Gravity can also be used to move the water from the cistern to the garden. If there is an adequate amount of elevation from where the cistern is placed to the garden, or positioning the cistern on a cement pad, gravity flow can be used, lowering the cost. Lastly, in order to "stretch" the collected water for food production, a drip irrigation system would be the best implementation. With a garden size of 150 m^2, the cost to set up a drip irrigation system would be approximately $72.

The total cost to implement a RWH system on the 4H building ranges from $3,204 - $11,973. The range is dependent on the cost of polyethylene cisterns, dependent on the manufacturer and age as well as the pump. Additional costs for RWH systems include maintenance which would require cleaning of the gutters before the start of the rainy season as well as a disinfecting method to ensure the prevention of bacteria growth.

Table 10 | Cost to implement a RWH system for the 4H building

Item	Size	Cost (USD)
Polyethylene Cisterns (2x)	29, 289 liters (7,737 gal)	$2,697 - $11,175
Gutter System	278 m^2 (2,990 ft^2)	$0
Pump	—	$435-$726
Drip Irrigation	150 m^2 (1,615 ft^2)	$72
Total Cost		**$3,204 - $11,973**

The cost to implement a rainwater harvesting system to collect water year-round would increase. For instance, additional cisterns would be needed to ensure that that the complete volume of precipitation is collected. The volume that can be collected year-round during a normal precipitation year is nearly double the amount that can be collected during the growing season at an average of 60,903 liters. Additionally, due to the cooler temperatures during the winter months, burial or insultation of the cisterns is required. Luckily, the cisterns can hold water for a long period of time if engineered to prevent sunlight from penetrating to avoid the growth of algae or bacteria. To start, it is suggested to implement a RWH for the growing season only, additional cisterns can be added to the system if more water is desired to be harvested throughout the year.

4.4 Climate Projections

The climate projections for Peach Springs are shown in Figure 26 and indicate an annual temperature increase from 1950 to 2099 for both moderate GHG emissions (green) and accelerated GHG (red). Additional climate projection plots can be found in the Appendix (8.1). Annual precipitation amounts, seen in Figure 27, have high variability and there is no observable pattern or trend for either GHG scenario. The number of dry days (Figure 28) shows a slight discernable increase for both GHG scenarios, suggesting that fewer precipitation days will occur.

The increase in temperature will increase ETo due to longer sunshine duration and increase in maximum temperature (Wang, 2020), which will require additional water to sustain a healthy crop yield. In addition, the increase in the number of dry days will reduce the amount of precipitation that is collected for RHW per month. If the annual amounts of precipitation do not change, but the number of dry days increase, then it follows that precipitation events might become less frequent, but the intensity of storms will increase. This might influence the feasibility of RWH in Peach Springs and across the Southwest.

The patterns of the North American monsoon (NAM) were not discerned from the climate projections since it was beyond the scope of this study. However, literature suggest, the monsoon will become more unpredictable. Pascale et al., (2017) suggests that the NAM will weaken as more atmospheric carbon dioxide is introduced, according the GCM simulations. The increase in warming temperature causes the disruption of the already sensitive NAM. In contrast, another study by Demaria et al., (2019) looking at 56

range gauge data throughout the Southwest from 1961-2017, show that there is an intensification in precipitation during the NAM. These contradictory findings suggest that a more research is needed to fully understand the characteristics of the NAM. This would require more rain gauges throughout the Southwest, as well as an increase in sensitivity in the GCMs (Demaria, et al., 2019).

Climate projections for Peach Springs show an earlier start to the growing season as well as a longer growing season in general due to the increase in temperatures (Appendix 8.1). This might also have an influence on the feasibility of RWH since the monsoon only occurs during the summer months of July-September. Crops grown before summer months would not benefit from monsoonal RWH, however, with half of the precipitation occurring throughout the rest of the year, crops could benefit from the stored water, assuring the feasibility. As shown, the months of May and June have the lowest average precipitation, so stored rainwater from the month of February would need to supplement the needs of the crops during an earlier growing season. With the earlier start and longer duration of the growing season, considering year-round rainwater harvesting is necessary.

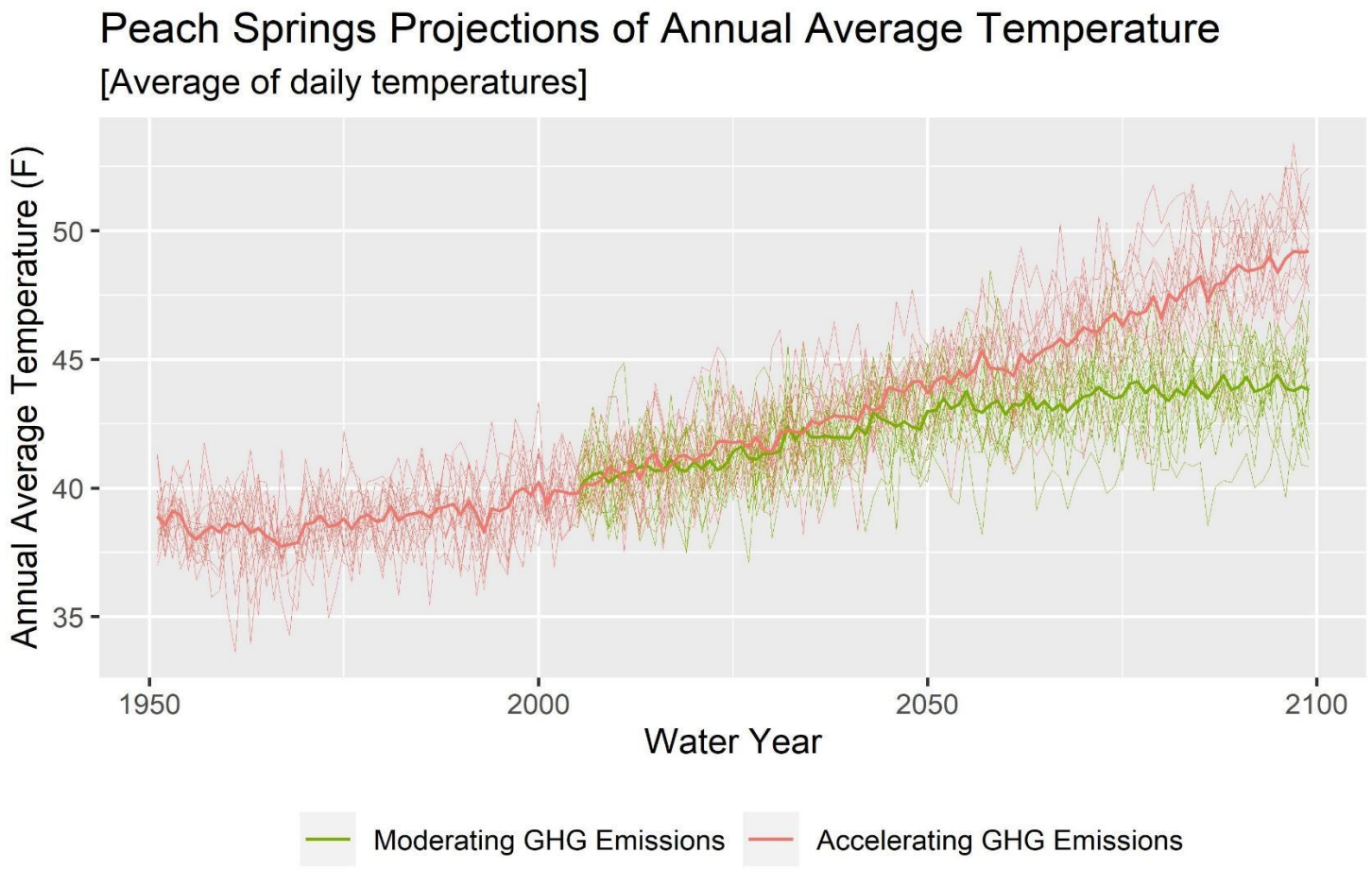

Figure 26 | Temperature projections show a clear increasing trend for the GHG emissions scenarios. Plot is in imperial units.

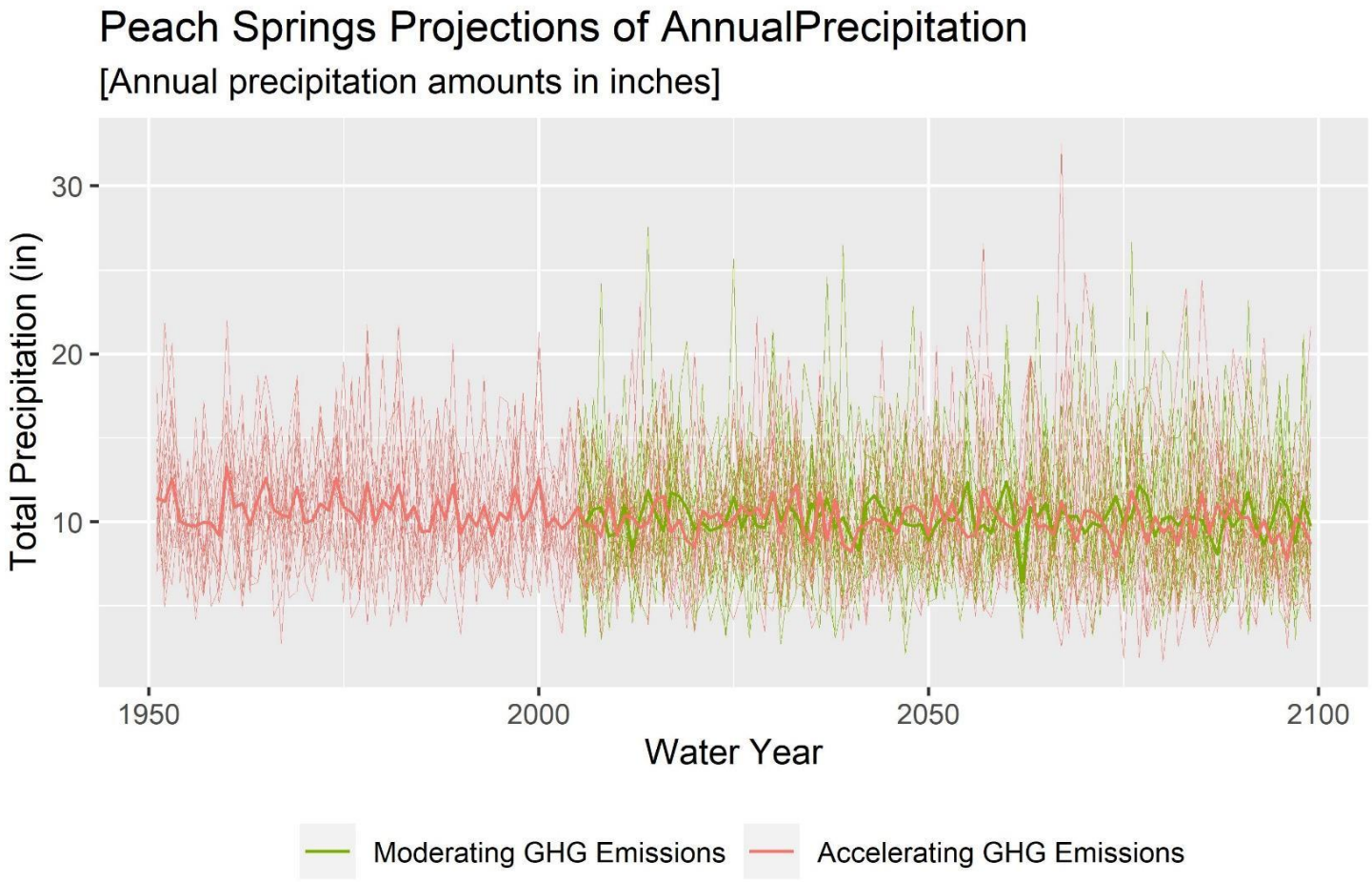

Figure 27 | Annual precipitation projections do not show a clear trend or change for either GHG emissions scenario. Plot is in imperial units.

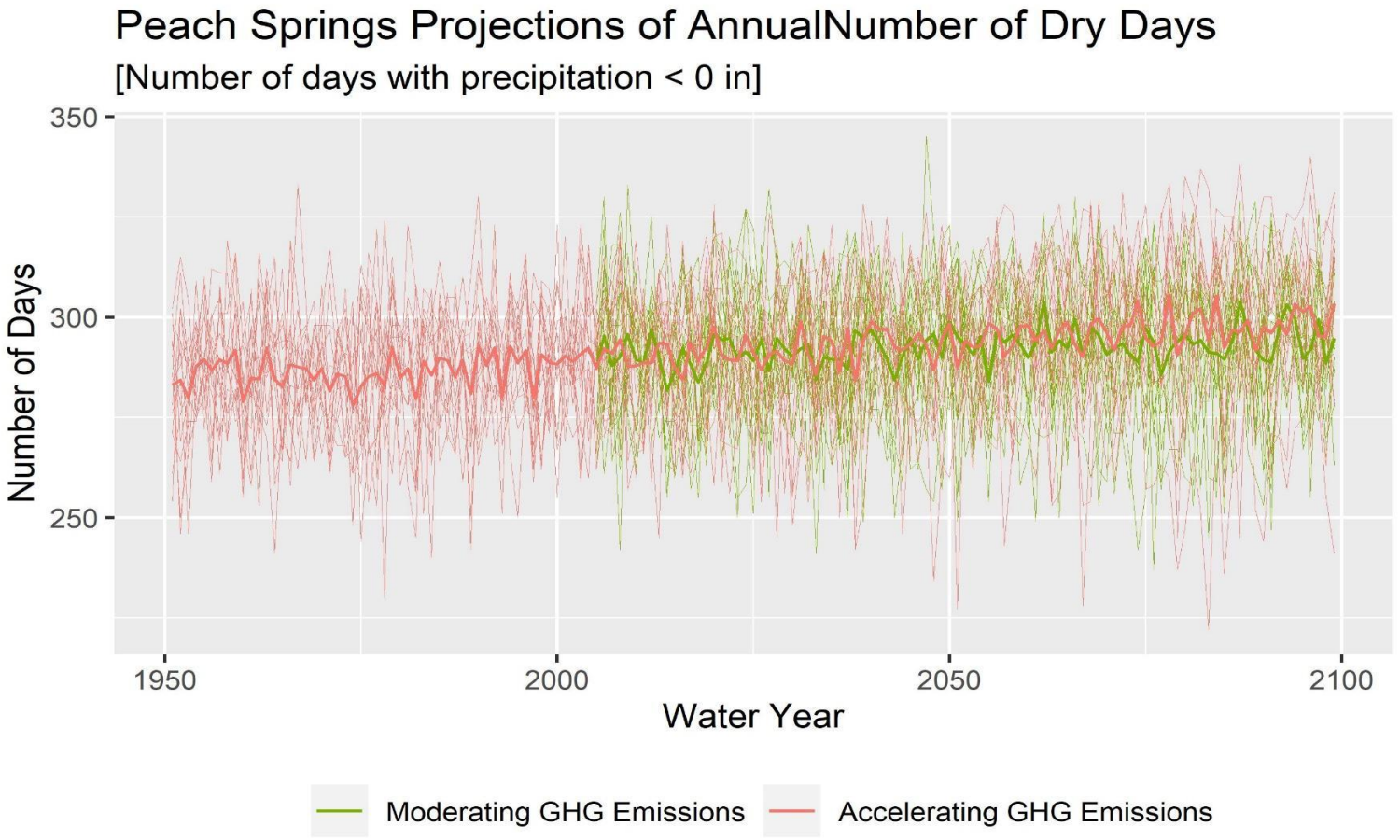

Figure 28 | Annual dry days projections show a clear increase of the number of dry days that will occur annually for the GHG emissions scenarios. Plot is in imperial units.

5.0 Social Impacts

Rainwater harvesting can help communities attain water security by improving water access and fulfilling demand (Malloy, 2020). Tribal communities in the US Southwest are discussing the need to become climate resilient, one of the greatest social challenges of the 21st century. It is crucial for these communities to secure water, not just for drinking, but for food production. Attaining food sovereignty is one of the components to becoming climate resilient and incredibly important during this unprecedented time, when a global pandemic has exposed the weaknesses in supply chains and our preparedness to combat COVID-19. Developing new water resources for food production could be beneficial for these communities.

Attaining food sovereignty can also help combat health problems (diabetes, heart disease, among other dietary illnesses) that disproportionately affect tribal and other rural communities. Growing healthy, culturally important food can be done using rainwater in the Southwest, where summer precipitation occurs. The Southwest has been cultivated for millennia by indigenous peoples, using successful techniques like RWH (Malloy, 2020).

Not only can RWH be implemented in rural communities, but in urban areas as well. The more rainwater harvesting and stormwater capture projects that are put into production, the less reliance on surface waters like the over-allocated Colorado River as well as critically over pumped aquifers like the Ogallala (Malloy, 2020). Cultivating

crops that are best adapted to these arid environments can also reduce the demand of water.

6.0 Conclusion

This study assessed the feasibility of rooftop RHW at a small scale, in Peach Springs, Arizona, on the Hualapai Indian Reservation. Three questions were specifically explored and addressed.

The current climate patterns support feasibility of RWH from four different buildings for food production. Using 40 years of precipitation and temperature data from PRISM Climate Group, an estimate of the harvestable water during a normal, dry, and wet year was determined from the four buildings. The FAO's AquaCrop model for maize, tomatoes, sunflowers, and dry beans, was used to determine the area that could be cultivated during the classified years, solely using the captured rainwater. Additionally, this study looked at future climate projections from CMIP 5 and existing literature for temperature and precipitation to further assess the feasibility of rainwater harvesting.

The existing rooftops on the four proposed are well-suited for rooftop RWH. The climate in Peach Springs makes it an ideal place to practice rooftop rainwater harvesting for food production. Although the volume of water that can be harvested from the 4H building and the Community Garden buildings cannot fully replace the irrigation practices that are currently in place, the harvested rainwater can help reduce the strain on current irrigation methods for various crops. The classification of precipitation years gives an average estimate of water that can be harvested during a normal, dry, and wet year.

Additionally, this study determined the land area can be cultivated using the harvested rainwater and whether a dry year is still sufficient to sustain the crops. The

harvested rainwater from the 4H building can help support more than one-third (40%) of the area that is being considered for cultivation during normal precipitation years, however, during a dry year the area that can be cultivated decreases to 35 m^2 (23%) of the area considered for cultivation, although significantly less, the water can still help support crops and reduce the strain on other irrigation methods. Classified wet years resulted in more precipitation availability during the winter months, December-February, however, additional engineering including burial or insulation of the cistern is required to avoid freezing of the water. Additionally, more cisterns will be needed to collect the maximum amount of precipitation, this would increase the cost of the RWH. Harvested rainwater can be stored in cisterns that are dark in color to block out the sunlight and prevent the growth of algae and bacteria, while simple and cost-effective disinfection methods (e.g., chlorination) can cease the growth of mosquitoes and microorganism in the stored water with 24 grams (0.85 oz) of calcium hypochlorite for every 3,785 liters (1000 gallons).

Climate projections along with existing literature, indicate that average annual temperature will continue to increase in the next few decades. Future precipitation trends are less clear. More variability and uncertainty surrounds climate projections involving precipitation to confidently conclude any trends. However, climate projections point towards an increase in dry days during a year, meaning days where 0 mm of precipitation occur. This indicates that it is expected for there to be more time between storms contributing to drought. However, when these storms occur, they will be stronger and less predictable. This would have an impact on the feasibility of rainwater harvesting in the Southwest. This requires the volume of cisterns to increase to be able to capture most of

the rain during these intense storms when present, however, this would also increase the cost of RWH.

Addressing water security will be one of the many challenges that all communities will face during this increase in temperature, however, some areas will be more challenging than others. In the Southwest, where summer precipitation occurs, rainwater harvesting can help mitigate these challenges. Capturing the water that would otherwise be lost to evaporation or evapotranspiration from unwanted plants, can help support small scale food production like community or domestic gardens. Attaining water security for food production is incredibly important, and more so with the changing climate. By expanding water resources in rural and tribal communities, food sovereignty can be attained. The amount of food that can be grown will depend on the catchment size in Peach Spring, AZ, and other similar communities in the Southwest.

7.0 Recommendations

Additional studies looking at the climate characteristics in northwestern Arizona would be useful in understanding why wet precipitation years (> 290 mm for Peach Springs) receive less water during the summer months when the North American Monsoon is present than the winter months during a water year. What mechanism is driving more precipitation during the winter months, but less precipitation during the summer months? How does this compare across the rest of the Southwest, if at all? Understanding why the summer storms lose intensity when there is a wet winter might be able to help farmers plant crops according to the water they will receive during the growing season. Additionally, looking at extremes in precipitation amounts would be beneficial to classify the precipitation years in more than just three categories over a longer timeframe. This would allow for more accurate representation of the harvestable amounts of rainwater. More importantly, looking at the NAM patterns to understand how it may be changing should also be consider since it is evident that there is no clear consensus among the literature.

Future studies looking at RWH should consider evaluating how much water can be collected at a domestic level for outdoor water use in a community. Can this volume help alleviate stresses on the current water resource in the community? Community outreach and incentives would be needed for rooftop rainwater harvesting to be implemented. It is also recommended for further research to look at which cultural foods grown in the Southwest can sustain warmer temperatures. These crops can be calibrated

and validated in AquaCrop to determine the area that can be cultivated using harvested rainwater.

8.0 Appendix

8.1 Results

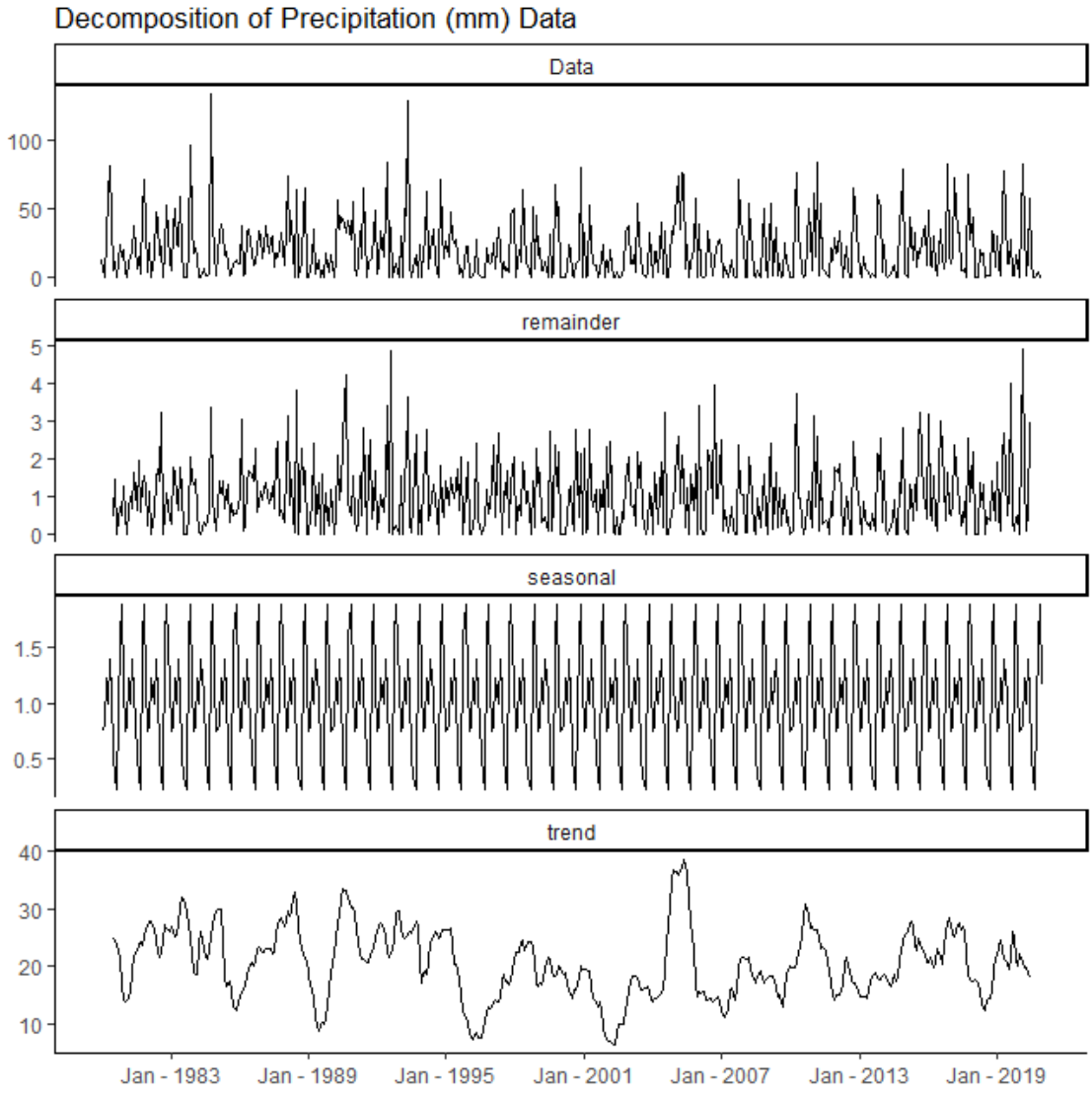

Figure 29 | Multiplicative decomposition of monthly precipitation time series from 1980- 2020 into three components: seasonality, trend, and the remainder (noise). Decomposition of a time series reduces the noise in the precipitation data and singles out the trend (Tt) for better interpretation of the data.

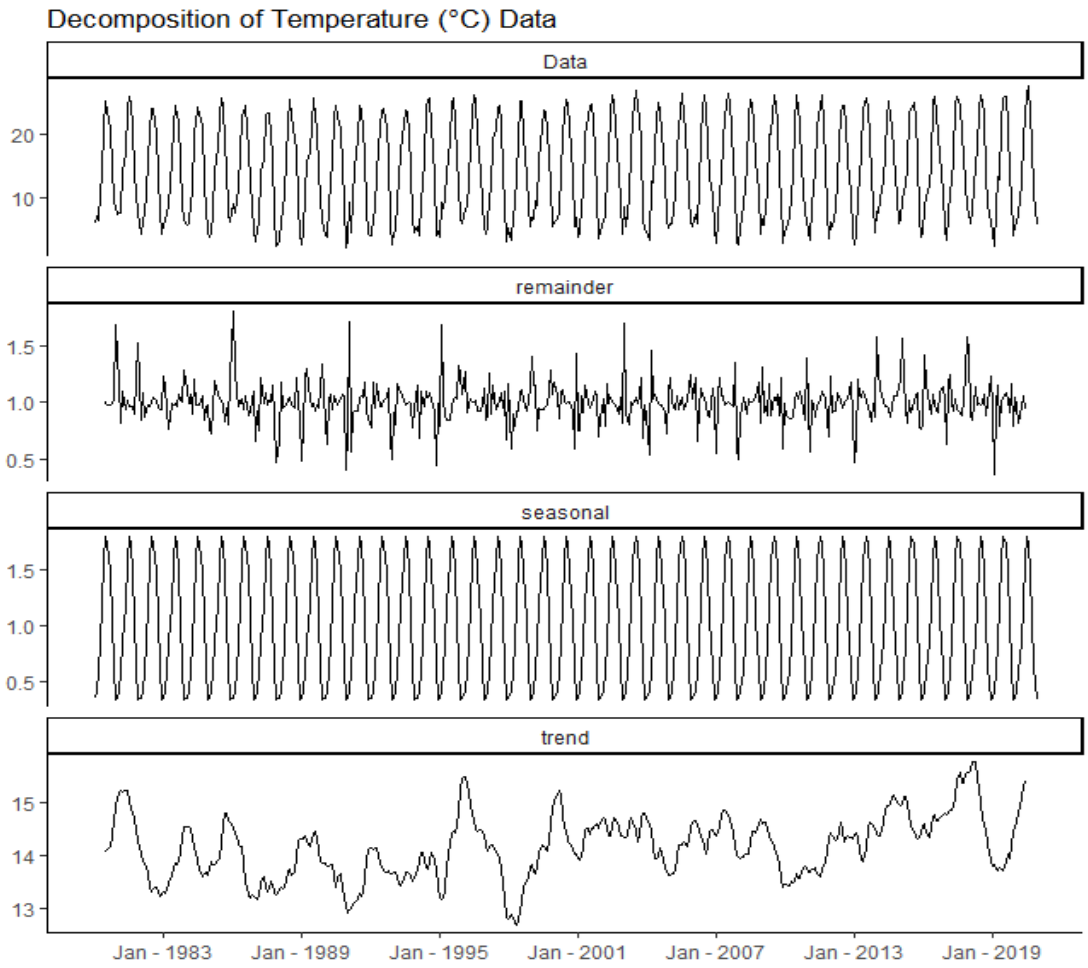

Figure 30 | Multiplicative decomposition of monthly temperature time series from 1980- 2020 into three components: seasonality, trend, and the remainder (noise). Decomposition of a time series reduces the noise in the temperature data and singles out the trend (Tt) for better interpretation of the data.

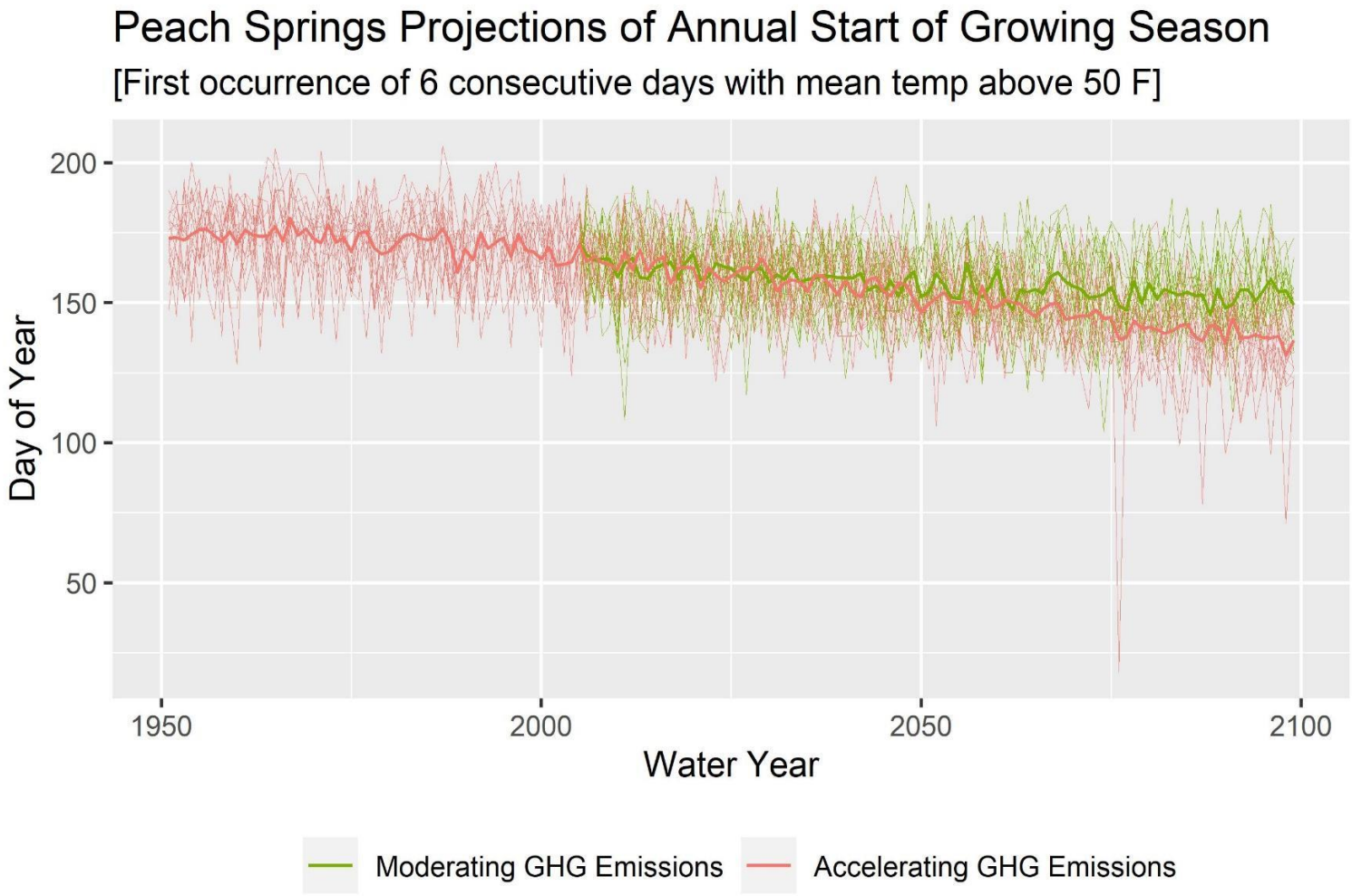

Figure 31 | Annual start of growing season seem to decrease to an earlier start in the year. Plot is in imperial units.

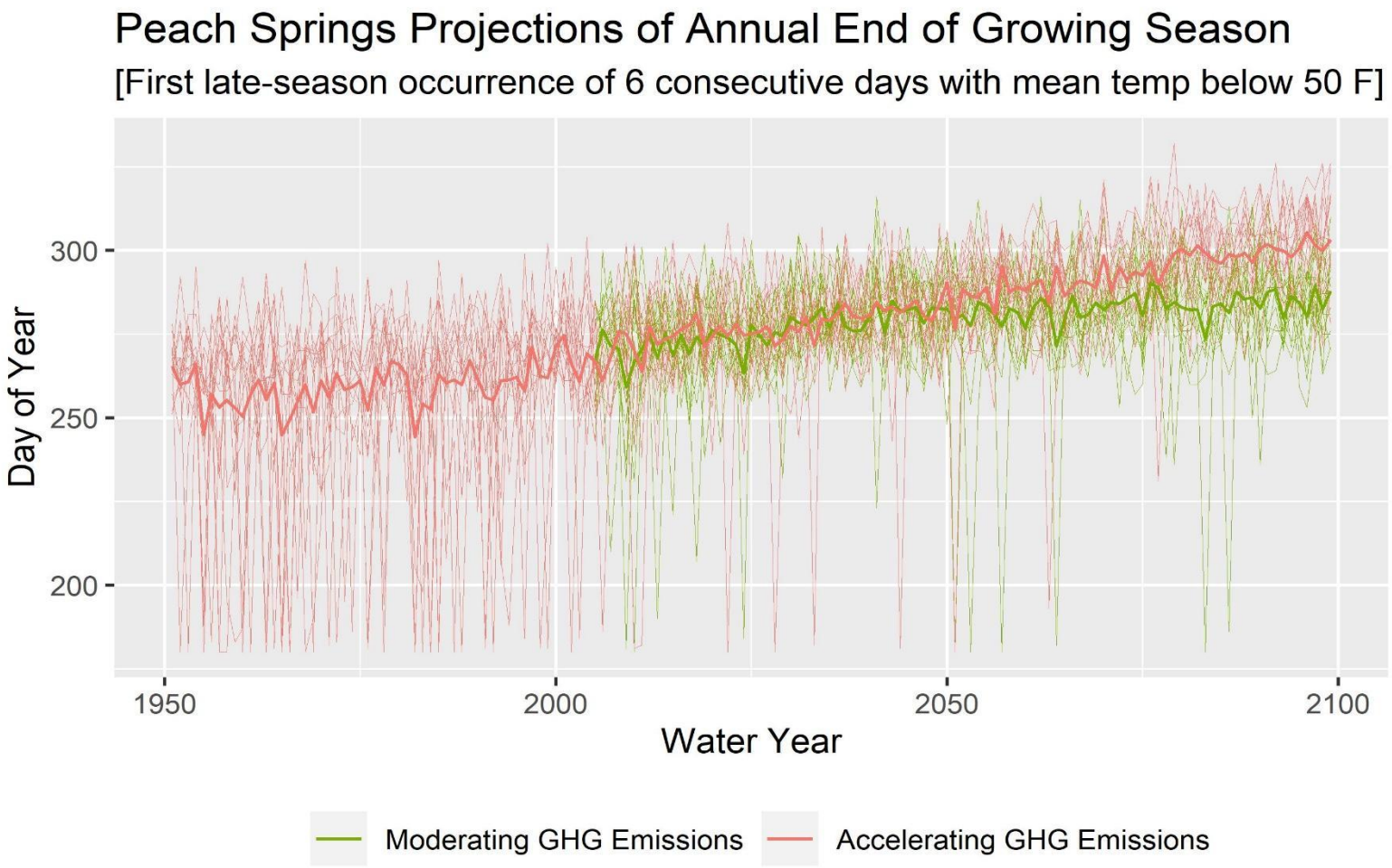

Figure 32 | Annual end to the growing season seems to arrive closer towards the end of the year. Plot is in imperial units

Figure 33 | Community Garden buildings (a.) Greenhouse (b.) Toolshed

Figure 34 | Hualapai Community Garden (a) SW view of the garden (b) NE view of garden. (c) Bean

Figure 35 | Other crops grown in the Hualapai Community Garden (a) Bell peppers (b) Yellow Squash. (c) Pepper. (d.) Gourd

Resources

Adams, D. K., & Comrie, A. C. (1997). *The North American Monsoon*. *7*(70), 18.

Aladenola, O. O., & Adeboye, O. B. (2010). Assessing the Potential for Rainwater Harvesting, Water Resources Management, 24(10), 2129–2137. https://doi.org/10.1007/s11269-009-9542-y

Allen, R.G., Pereira, L.S., Raes, D., Smith, M., (1998) Crop evapotranspiration - Guidelines for computing crop water requirements - FAO Irrigation and drainage paper 56, FAO- Food and Agriculture Organization of the United Nations, Rome. Retrieved from: https://www.fao.org/3/X0490E/x0490e00.htm#Contents

Arvind, G., Ashok Kumar, P., Girish Karthi, S., & Suribabu, C. R. (2017). Statistical Analysis of 30 Years Rainfall Data: A Case Study. IOP Conference Series: Earth and Environmental Science, 80, 012067. https://doi.org/10.1088/1755-1315/80/1/012067

Bills, D.J., and Macy, J.P., 2016, Hydrologic framework and characterization of the Truxton aquifer on the Hualapai Reservation, Mohave County, Arizona (ver. 2.0, December 2017): United States Geological Survey Scientific Investigations Report 2016–5171, 50 p., https://doi.org/10.3133/sir20165171

Blue Bird Jernigan, V., Salvatore, A. L., Styne, D. M., & Winkleby, M. (2012). Addressing food insecurity in a Native American reservation using community-based participatory research. Health Education Research, 27(4), 645–655. https://doi.org/10.1093/her/cyr089

Christensen, K., & Hualapai Tribe Department of Natural Recourses (HTDNR), (2003), Cooperative Drought Contingency Plan, Hualapai Reservation. Retrieved from: https://drought.unl.edu/archive/plans/drought/Tribal/HualapaiTribe_2003.pd

Coleman-Jensen, A., Rabbitt, M. P., Gregory, C. A., & Singh, A. (2020) Household Food Security in the United States in 2020, ERR-298, U.S. Department of Agriculture, Economic Research Service.

Copeland, S. M., J. B. Bradford, M. C. Duniway, and R. M. Schuster. 2017. Potential impacts of overlapping land-use and climate in a sensitive dryland: a case study of the Colorado Plateau, USA. Ecosphere 8(5):e01823. 10.1002/ecs2.1823

Congressional Research Service, Casey, A.R., & Morgenstern E. M. (2020) Covid-19 and Global Food Security: Issues for Congress. In Focus. Retrieved from: https://crsreports.congress.gov/product/pdf/IF/IF11575

Crimmins, A. (2006). Arizona and the North American Monsson System. *Arizona Cooperative Extension.* College of Agriculture and Life Sciences, University of Arizona (Tucson, AZ). https://repository.arizona.edu/handle/10150/146919

Demaria, E. M. C., Hazenberg, P., Scott, R. L., Meles, M. B., Nichols, M., & Goodrich, D. (2019). Intensification of the North American Monsoon Rainfall as Observed From a Long-Term High-Density Gauge Network. Geophysical Research Letters, 46(12), 6839–6847. https://doi.org/10.1029/2019GL082461DeMeo, J. (1991). OROP ARIZONA 1989: A Cloudbusting Experiment To Bring Rains in the Desert Southwest.

DigDeep and US Water Alliance (2020). Closing the Water Access Gap in the United States: A National Action Plan, Los Angeles, CA. Retrieved from: https://www.closethewatergap.org/wp-content/uploads/2019/11/Dig-Deep_Closing-the-Water- Access-Gap-in-the-United-States_EXECUTIVE-SUMMARY-1.pdf

Dingman, L., (2015) Physical Hydrology, third Edition. Waveland Press, INC. Long Grove, Illinois.

Dominguez, F., Miguez-Macho, G., & Hu, H. (2016). WRF with Water Vapor Tracers: A Study of Moisture Sources for the North American Monsoon. *Journal of Hydrometeorology*, *17*(7), 1915–1927. https://doi.org/10.1175/JHM-D-15-0221.1

Durodola, O. S., Bwambale, J., & Nabunya, V. (2020). Using every drop: Rainwater harvesting for food security in Mbale, Uganda. Water Practice and Technology, 15(2), 295–310. https://doi.org/10.2166/wpt.2020.019

Food and Agriculture Organization (FAO) Division of Land and Water (2022). ETo Calculator, Retrieved from: https://www.fao.org/land-water/databases-and-software/eto-calculator/en/

Garfin G, Jardine A, Merideth R, Black M, LeRoy S (2013) Assessment of climate change in southwest United States: a report prepared for the National Climate Assessment. Island Press, Washington DC.

Garg, K. K., Anantha, K. H., Venkataradha, A., Dixit, S., Singh, R., & Ragab, R. (2021). Impact of Rainwater Harvesting on Hydrological Processes in a Fragile Watershed of South Asia. Groundwater, 59(6), 839–855. https://doi.org/10.1111/gwat.13099

Ghisi, E. (2006). Potential for potable water savings by using rainwater in the residential sector of Brazil. Building and Environment, 41(11), 1544–1550. https://doi.org/10.1016/j.buildenv.2005.03.018

Ghisi, E., Bressan, D. L., & Martini, M. (2007). Rainwater tank capacity and potential for potable water savings by using rainwater in the residential sector of southeastern Brazil. Building and Environment, 42(4), 1654–1666. https://doi.org/10.1016/j.buildenv.2006.02.007

Guarino, J. (2015). Tribal Food Sovereignty in the American Southwest. Journal of Food Law and Policy, 11(1), 83-112.

Helsel, D.R., Hirsch, R.M., Ryberg, K.R., Archfield, S.A., and Gilroy, E.J. (2020) Statistical methods in water resources: United States Geological Survey Techniques and Methods, book 4, chapter A3, 458 p., https://doi.org/10.3133/tm4a3. [Supersedes USGS Techniques of Water-Resources Investigations, book 4, chapter A3, version 1.1.]

Hsiao, T. C., & Bongiovanni, M. (n.d.). *3.4 Herbaceous crops*. 155. Retrieved from: https://www.fao.org/3/i2800e/i2800e07.pdf

Hualapai Department of Cultural Resources (HDCR) (2010) About the Hualapai Nation Booklet Retrieved from: http://hualapai-nsn.gov/wp-content/uploads/2011/05/AboutHualapaiBooklet.pdf

Hualapai Department of Natural Resources (HDNR) (2004) Hualapai Tribe Pre-Disaster Mitigation Plan. Retrieved from: http://hualapai-nsn.gov/wp-content/uploads/2015/05/2004-Hualapai-Fema-Mitigation-Plan.pdf

Indian Meteorological Department (IMD) (2022) Ministry of Earth Sciences, Government of India, Frequently Asked Questions (FAQs) on Monsoon. Retrieved from https://mausam.imd.gov.in/imd_latest/monsoonfaq.pdf

Jana, S., Rajagopalan, B., Alexander, M. A., & Ray, A. J. (2018). Understanding the Dominant Sources and Tracks of Moisture for Summer Rainfall in the Southwest United States. *Journal of Geophysical Research: Atmospheres*, *123*(10), 4850-4870.https://doi.org/10.1029/2017JD027652

Kamworapan, S., & Surussavadee, C. (2019). Evaluation of CMIP5 Global Climate Models for Simulating Climatological Temperature and Precipitation for Southeast Asia. Advances in Meteorology, 2019, 1–18. https://doi.org/10.1155/2019/1067365

Kohler, M.A., Nordenson, T.J., and Baker, D.R., 1959, Evaporation maps for the United States: Department of Commerce, Weather Bureau, Technical Paper no. 37, 13 p.

Kummu, M., Ward, P.J., de Moel, H., Varis, O., (2010). Is physical water scarcity a new phenomenon? Global assessment of water shortage over the last two millennia. Environment Research Letter 5 (034006), 10 doi: 1748-9326/10/034006.

Lasage, R., Verburg, P.H., (2015). Evaluation of small-scale water harvesting techniques for semi-arid environments. Journal of Arid Environments 118, 48-57, doi: https://doi.org/10.1016/j.jaridenv.2015.02.019

La Vía Campesina. 2007. Declaration of Nyéléni. La Vía Campesina International Peasant's Movement. 27 February. https://viacampesina.org/en/declaration-of-nyi/.

Leonard, D., (2021) Monsoon brings welcome rain to the Southwest, but drought stubbornly persists. The Washington Post. July 29, 2021.

Livneh B., E.A. Rosenberg, C. Lin, B. Nijssen, V. Mishra, K.M. Andreadis, E.P. Maurer, and D.P. Lettenmaier, 2013: A Long-Term Hydrologically Based Dataset of Land Surface Fluxes and States for the Conterminous United States: Update and Extensions, Journal of Climate, 26, 9384–9392.

Lynn, E., Chair, C., O'Daly, W., Keeley, F., Dsiwm, D., Woled, J., & Dsiwm, D. (2015). California Department of Water Resources (DWR) Climate Change Technical Advisory Group (CCTAG). 142

Malloy, C., (2020) Millions of Americans lack access to running water. An ancient method of capturing rainwater can help solve this. The Counter. Retrieved from: https://thecounter.org/ancient-rainwater-harvest-technology-used-for-access-to-water-supply-navajo-nation/

Mason, J.P., Knight, J.E., Ball, L.B. Kennedy, J.R., Bills, D.J., and Macy, J.P., (2020), (a) Groundwater availability in the Truxton basin, northwestern Arizona, chap. A of Mason, J.P., ed., Geophysical surveys, hydrogeologic characterization, and groundwater flow model for the Truxton basin and Hualapai Plateau, northwestern Arizona: U.S. Geological Survey Scientific Investigations Report 2020–5017, 14 p., https://doi.org/10.3133/sir20205017A.

Mason, J.P., Bills, D.J., and Macy, J.P., (2020) (b) Geology and hydrology of the Truxton basin and Hualapai Plateau, northwestern Arizona, chap. B of Mason, J.P., ed., Geophysical surveys, hydrogeologic characterization, and groundwater flow model for the Truxton basin and Hualapai Plateau, northwestern Arizona: U.S. Geological Survey Scientific Investigations Report 2020–5017, 9 p., https://doi.org/10.3133/sir20205017B.

Mekonnen, M.M., Hoekstra, A.Y., (2016). Four billion people facing severe water scarcity. Science Advances 2(2): e1500323. doi: 10.1126/sciadv.1500323

Myers, A. M., & Painter, M. A. (2017). Food insecurity in the United States of America: An examination of race/ethnicity and nativity. Food Security, 9(6), 1419–1432. https://doi.org/10.1007/s12571-017-0733-8

National Park Service (2021) Peach Springs Trading Post, Peach Springs, Arizona. Retrieved from: https://www.nps.gov/nr/travel/route66/peach_springs_trading_post.html

Pascale, S., Boos, W. R., Bordoni, S., Delworth, T. L., Kapnick, S. B., Murakami, H., Vecchi, G. A., & Zhang, W. (2017). Weakening of the North American monsoon with global warming. *Nature Climate Change*, *7*(11), 806–812. https://doi.org/10.1038/nclimate3412

Pierce, D. W., Cayan, D. R., & Thrasher, B. L. (2014). Statistical Downscaling Using Localized Constructed Analogs (LOCA), Journal of Hydrometeorology, 15(6), 2558-2585. Retrieved Apr 28, 2022, from https://journals.ametsoc.org/view/journals/hydr/15/6/jhm-d-14-0082_1.xm

Pindus, N., & Hafford, C. (2019). Food security and access to healthy foods in Indian country: Learning from the Food Distribution Program on Indian Reservations. Journal of Public Affairs, 19(3). https://doi.org/10.1002/pa.1876

Power, T., et. al. (2020). COVID-19 and Indigenous Peoples: An imperative for action. Journal of Clinical Nursing, vol. 29, Issues: 15-16, pages: 2737-2741. https://doiorg.unr.idm.oclc.org/10.1111/jocn.15320

PRISM Climate Group, Oregon State University, http://prism.oregonstate.edu, created 4 Feb 2004, accessed August 2021 https://prism.oregonstate.edu

Raes, D. (2012) The ETo Calculator, Reference Manual, version 3.2., Food and Agriculture Organization of the United Nations Land and Water Division. Rome, Italy. Retrieved from: https://www.ipcinfo.org/fileadmin/user_upload/faowater/docs/ReferenceManualV32.pdf

Rodriguez-Lonebear, D. (2016). Building a data revolution in Indian Country. In T. Kukutai, &. J.Taylor (Eds.), Indigenous Data Sovereignty: toward an agenda (pp. 253-272). Acton, Australia: ANU press.

Sheffield, J., Barrett, A. P., Colle, B., Nelun Fernando, D., Fu, R., Geil, K. L., Hu, Q., Kinter, J., Kumar, S., Langenbrunner, B., Lombardo, K., Long, L. N., Maloney, E., Mariotti, A., Meyerson, J. E., Mo, K. C., David Neelin, J., Nigam, S., Pan, Z., … Yin, L. (2013). North American Climate in CMIP5 Experiments. Part I: Evaluation of Historical Simulations of Continental and Regional Climatology. Journal of Climate, 26(23), 9209–9245. https://doi.org/10.1175/JCLI-D-12-00592.1

Steduto, P., Hsiao, T. C., Raes, D., & Fereres, E. (2009). AquaCrop-The FAO Crop Model to Simulate Yield Response to Water: I. Concepts and Underlying Principles. Agronomy Journal, 101(3), 426–437. https://doi.org/10.2134/agronj2008.0139s

Steele, C., Reyes, J., Elias, E., Aney, S., & Rango, A. (2018). Cascading impacts of climate change on southwestern US cropland agriculture. Climatic Change, 148(3), 437–450. https://doi.org/10.1007/s10584-018-2220-4

Stenner., H.D., Lund, W.R.., Pearthree, P.A., Everitt, B.L. (1999) Paleoseismologic Investigations of the Hurricane Fault in Northwestern Arizona and Southwestern Utah. Arizona Geological Survey Open File Report 99-8. http://repository.azgs.az.gov/sites/default/files/dlio/files/2010/u14/OFR99-8Hurricanefault.pdf

Tamaddun, K., Kalra, A., & Ahmad, S. (2018). Potential of rooftop rainwater harvesting to meet outdoor water demand in arid regions. Journal of Arid Land, 10(1), 68–83. https://doi.org/10.1007/s40333-017-0110-7

Texas Water Development Board (2005). The Texas Manual on Rainwater Harvesting. 3rd Edition. Austin Texas

Quezadas, J. P., Adams, D., Sánchez Murillo, R., Lagunes, A. J., & Rodríguez Castañeda, J. L (2021). Isotopic variability (δ18O, δ2H and d-excess) during rainfall events of the north American monsoon across the Sonora River Basin, Mexico. *Journal of South American Earth Sciences*, *105*, 102928. https://doi.org/10.1016/j.jsames.2020.102928

University of Arizona-Tucson (UA) (2021) Hualapai Tribe. The Native Peoples Technical Assistance Office. https://nptao.arizona.edu/hualapai-tribe.

Van Meter, K.J., Steiff, M., McLaughlin, D.L., Basu, N.B., (2016) The socioecohydrology of rainwater harvesting in India: understanding water storage and release dynamics across spatial scales. Hydrol. Earth Syst. Sci., 20, 2629–2647, doi:10.5194/hess-20-2629-201

Vanuytrecht, E., Raes, D., Steduto, P., Hsiao, T. C., Fereres, E., Heng, L. K., Garcia Vila, M., & Mejias Moreno, P. (2014). AquaCrop: FAO's crop water productivity and yield response model. Environmental Modelling & Software, 62, 351–360. https://doi.org/10.1016/j.envsoft.2014.08.005

Wang, J., & Schmidt, J. C. (2020). Stream flow and Losses of the Colorado River in the Southern Colorado Plateau. 26.

Wang, K., Xu, Q., & Li, T. (2020). Does recent climate warming drive spatiotemporal shifts in functioning of high-elevation hydrological systems? Science of The Total Environment, 719, 137507. https://doi.org/10.1016/j.scitotenv.2020.137507

Warne, D., & Wescott, S. (2019.). Social Determinants of American Indian Nutritional Health. CURRENT DEVELOPMENTS IN NUTRITION, 7.

Western Regional Climate Center. (2021). Cooperative Climatological Data Summaries. Retrieved from https://wrcc.dri.edu/cgi-bin/cliMAIN.pl?az6328

Williams, A. P., Cook, B. I., & Smerdon, J. E. (2022). Rapid intensification of the emerging southwestern North American megadrought in 2020–2021. Nature Climate Change. https://doi.org/10.1038/s41558-022-01290-z

Wilson, N. J., Montoya, T., Arseneault, R., & Curley, A. (2021). Governing water insecurity: Navigating indigenous water rights and regulatory politics in settler colonial states. Water International, 1–19. https://doi.org/10.1080/02508060.2021.1928972